



1 **Vista-LA: Mapping methane emitting infrastructure in the Los** 2 **Angeles megacity**

3

4 Valerie Carranza^{1,2}, Talha Rafiq^{1,3}, Isis Frausto-Vicencio^{1,4,*}, Francesca Hopkins^{1,*}, Kristal R. Verhulst^{1,3},
5 Preeti Rao^{1,**}, Riley M. Duren¹, Charles E. Miller¹

6 ¹ Jet Propulsion Laboratory, California Institute of Technology, Pasadena, CA, 91109, U.S.A.

7 ² Institute of the Environment and Sustainability, University of California, Los Angeles, Los Angeles,
8 CA, 90024, U.S.A.

9 ³ Joint Institute for Regional Earth System Science and Engineering, University of California, Los
10 Angeles, CA, 90024, U.S.A.

11 ⁴ Department of Chemistry, University of California, Los Angeles, Los Angeles, CA 90024, U.S.A.

12 * Now at: University of California, Riverside, Riverside, CA, 92521 U.S.A.

13 **Now at: University of Michigan, Ann Arbor, MI 48109 U.S.A.

14 *Correspondence to:* Kristal Verhulst (Kristal.R.Verhulst@jpl.nasa.gov)

15 **Abstract**

16

17 Methane is a potent greenhouse gas (GHG) and a critical target of climate mitigation efforts. However,
18 actionable emission reduction efforts are complicated by large uncertainties in the methane budget at
19 relevant scales. Here, we present Vista, a Geographic Information System (GIS)-based approach to map
20 potential methane emissions sources in greater Los Angeles, an area with a dense, complex mixture of
21 sources. The goal of this work is to provide a database that, together with atmospheric observations,
22 improves methane emissions estimates in urban areas with complex infrastructure. We aggregated
23 methane source location information into three sectors (energy, agriculture, and waste) following the
24 frameworks used by the State of California GHG Inventory and the IPCC Guidelines for GHG Reporting.
25 Geospatial modelling was applied to publicly available datasets to precisely geolocate facilities and
26 infrastructure comprising major anthropogenic methane source sectors. The final database, Vista-Los
27 Angeles (LA), is presented as maps of infrastructure known or expected to emit methane. Vista-LA



28 contains over 33,000 features concentrated on <1% of land area in the region. Currently, Vista-LA is used
29 as a planning and analysis tool for atmospheric measurement surveys of methane sources, particularly for
30 airborne remote sensing, and methane “hot-spot” detection using regional observations. This study
31 represents a first step towards developing an accurate, spatially-resolved methane flux estimate for point
32 sources in California’s South Coast Air Basin (SoCAB), with the potential to address discrepancies
33 between bottom-up and top-down methane emissions accounting. The final Vista-LA datasets and
34 associated metadata have been submitted to the Oak Ridge National Laboratory Distributed Active
35 Archive Center for Biogeochemical Dynamics (ORNL DAAC;
36 <https://doi.org/10.3334/ORNLDAAC/1525>).



37 **1 Introduction**

38 Methane (CH₄) is the second most important anthropogenic driver of climate change (Myhre et al., 2013).
39 Recent studies have shown that mitigating CH₄ emissions yields large near-term climate benefits due to
40 CH₄'s relatively short atmospheric lifetime (Dlugokencky et al., 2011). Reducing CH₄ emissions is
41 complicated by the incomplete understanding of the CH₄ budget at scales relevant to actionable emissions
42 reduction efforts. Cities are important for GHG mitigation, since they represent high-density emissions
43 regions with the appropriate scale to reduce GHG emissions (Duren and Miller, 2012; Kennedy et al.,
44 2009). Additionally, political will and commitment is needed to implement mitigation efforts for reducing
45 GHG emissions (Gurney et al., 2015). However, enacting emission controls is challenging in urban areas
46 that are highly complex and heterogeneous, with various emission sources located in close proximity.

47 Understanding urban emissions requires knowledge of source sectors and their respective activities at
48 scales that align with urban policy and planning (typically 10's to 100's of meters). Such information has
49 been assembled for fossil fuel carbon dioxide (CO₂) emissions using the Hestia approach, which
50 quantifies urban sources down to the building level (Gurney et al., 2012). To date, Hestia has generated
51 detailed estimates of urban CO₂ emissions for several cities, including Los Angeles (LA) (Rao et al., *in*
52 *review*), Indianapolis (Gurney et al., 2012), and Salt Lake City (Patarasuk et al., 2016). A CH₄ emissions
53 product with spatial information equivalent to the scale of Hestia is needed for CH₄ emissions mitigation
54 efforts. However, the sources of CH₄ differ significantly from those of CO₂, which are primarily driven
55 by fossil fuel combustion. Therefore, the methods used to develop Hestia are not directly transferable to
56 CH₄, which has distinct source processes and spatial patterns from CO₂.

57 Urban areas are globally significant sources of CH₄ emissions, primarily coming from energy use and
58 waste management (Hopkins et al., 2016a; Marcotullio et al., 2013). However, knowledge of the location
59 and relative contribution of these emission sources is highly uncertain, especially in urban areas where
60 energy, waste treatment, and other CH₄ emission sources are located in close proximity to one another.
61 Global emissions inventories based on nightlights and/or population scaling methods (e.g., EDGAR v4.2
62 European Commission Joint Research Centre, 2010; Olivier and Peters, 2005) are limited in their
63 usefulness for estimating emissions at the scale of a city or air basin. Official CH₄ emission inventories



64 made using bottom-up approaches (e.g., IPCC, 2006) underestimate CH₄ emissions and are driven by a
65 different mixture of sources compared to those inferred from atmospheric measurements, as observed in
66 Los Angeles (Hopkins et al., 2016b; Hsu et al., 2009; Townsend-Small et al., 2012; Wennberg et al.,
67 2012; Wong et al., 2016, 2015; Wunch et al., 2009), Boston (McKain et al., 2015), Indianapolis
68 (Cambaliza et al., 2015), Florence (Gioli et al., 2012), London (Helfter et al., 2016), and San Francisco
69 (Jeong et al., 2017)). Consequently, there is a need for a new approach of urban CH₄ assessment that
70 overcomes these shortcomings by incorporating both top-down (observation-based) and bottom-up
71 (activity-based) information.

72 Atmospheric CH₄ in the urban landscape is dominated by CH₄ hotspots that primarily come from fossil
73 fuel-derived sources (e.g., Hopkins et al., 2016b). Many of these hotspots are associated with leaks—
74 fugitive CH₄ emissions—in natural gas systems (e.g., Jackson et al., 2014; Phillips et al., 2013). Across
75 the natural gas infrastructure, CH₄ emissions are disproportionately emitted by a small fraction of “super-
76 emitters” (Brandt et al., 2014). Fugitive CH₄ emissions sources are more challenging to inventory than
77 activity-related emissions, and contribute to uncertainty in the magnitude and spatial pattern of CH₄
78 emissions in urban areas (Hopkins et al., 2016b; Lamb et al., 2015). In recent studies, the locations of
79 fugitive emissions have been identified using observational data, such as mobile surveys, airborne
80 campaigns, and sustained monitoring (e.g., Cambaliza et al., 2015; Frankenberg et al., 2016; Hopkins et
81 al., 2016b; Verhulst et al., 2017).

82 Inaccuracies and coarse information in city-scale inventories of CH₄ pose a direct obstacle to city
83 mitigation plans. Shortcomings in bottom-up methods have been identified to be: inaccurate
84 representation of fugitive CH₄ sources at fine spatial scales, the existence of unreported CH₄ sources in
85 urban areas, and/or incomplete accounting of known CH₄ sources, such as from oil and gas activities
86 (Hopkins et al., 2016a; Lyon et al., 2015; Zavala-Araiza et al., 2015). CH₄ emissions estimates for urban
87 regions can be improved by more complete accounting of potential CH₄ sources at the facility scale, along
88 with targeted observations that can detect fugitive emissions and super-emitter behavior.



89 Here, we present Vista, a GIS-based CH₄ emissions mapping database designed to address shortcomings
90 in current urban CH₄ inventories. Vista encompasses key CH₄ emissions categories from the
91 Intergovernmental Panel on Climate Change (IPCC) GHG Inventory methodology. The primary goal of
92 this research effort is to improve understanding of CH₄ emissions at urban scales with complex mixtures
93 of sources, exemplified by the LA Megacity. Emissions monitoring and verification efforts in LA are
94 highly relevant for California's statewide emissions control efforts. The LA Megacity emits a significant
95 fraction of California's GHG emissions, with 42% of the state's population concentrated in 4% of the
96 state's land area (CARB, 2014b).

97 In this study, we present the Vista-LA database for the spatial domain of California's South Coast Air
98 Basin (SoCAB), the air basin that contains the majority of LA Megacity GHG emissions. Vista-LA
99 consists of detailed spatial maps for facilities and infrastructure in the SoCAB that are known or expected
100 sources of CH₄ emissions. Vista-LA illustrates the spatial distribution of potential CH₄ sources,
101 representing a first step towards developing an urban-scale CH₄ emissions gridded inventory for the
102 SoCAB. The final Vista-LA database contains over 33,000 entries, which are presented as CH₄ emitting
103 infrastructure maps. SoCAB is an ideal testbed due to the density of sources and availability of
104 observations from the LA Megacity Carbon Project (<https://megacities.jpl.nasa.gov/portal/>) tower
105 network (Newman et al., 2016; Verhulst et al., 2017), the California Laboratory for Atmospheric Remote
106 Sensing (CLARS) (Wong et al., 2016, 2015), and a total column carbon observing network site (Wunch
107 et al., 2009). The Vista data product is a key tool for CH₄ emissions research and mitigation efforts; by
108 (1) mapping areas of CH₄ emitting infrastructure, (2) identifying targets for CH₄ surveys, and (3) enabling
109 interpretation of atmospheric observations, including source attribution, and comparison of measured
110 emissions to permitted or reported emissions. Combined with atmospheric observations, Vista enables
111 systematic study of urban CH₄ emission sources.

112



113 **2 Methods Overview**

114 **2.1 Vista-LA Structure and Organization**

115 The spatial domain for the Vista-LA database is SoCAB, the air-shed for the greater Los Angeles urban
116 extent, including the urbanized parts of Los Angeles, Orange, Riverside, and San Bernardino Counties.
117 Vista-LA follows the IPCC CH₄ emissions reporting framework (IPCC, 2006). Following IPCC
118 methodology provides compatibility with the State of California CH₄ emissions inventory and allows the
119 approach used in this study to be adapted to other regions globally (CARB, 2014a, 2015). For example,
120 Vista-LA can be easily adapted to the Environmental Protection Agency (EPA) national inventory
121 structure since it also follows the 2006 IPCC Guidelines for National GHG Inventories as shown in Figure
122 A1 (EPA, 2016).

123 The Vista-LA structure enables sectoral tracking of emissions. We used the State of California GHG
124 Inventory for 2015 (CARB, 2016), the most policy-relevant inventory that includes the SoCAB domain,
125 to rank the top CH₄ emitting sources (Figure 1). According to the State of California GHG Inventory,
126 ~99% of California's CH₄ emissions are expected to result from just three IPCC Level 1 categories –
127 energy, agriculture, and waste, and eight IPCC Level 3 categories – fuel combustion activities related to
128 energy industries and transport (IPCC – 1A1 & 1A3), fugitive emissions related to oil and natural gas
129 (IPCC – 1B2), livestock emissions related to enteric fermentation (IPCC – 3A1) and manure management
130 (IPCC – 3A2); and solid and liquid waste disposal and treatment, including managed waste disposal sites
131 (4A1), and domestic and industrial wastewater treatment and discharge facilities (IPCC – 4D1 & 4D2,
132 respectively) (see Figure 1). The other 27 Level 3 categories cumulatively contribute less than 1% of
133 California's CH₄ emissions, and are hence assumed to have negligible impact on SoCAB CH₄ emissions.
134 This approach greatly simplifies the database, allowing us to focus our attention on the top-emitting
135 sources. By design, Vista-LA only includes Scope 1 emissions—that is, direct GHG emissions from
136 sources that are owned or controlled by a company within the study domain, as defined by the GHG
137 Protocol (<http://www.ghgprotocol.org/corporate-standard>). Therefore, sources that are not expected to
138 result in significant direct emissions of CH₄ in the SoCAB were excluded, such as emissions from
139 imported electricity, geothermal energy production, and from solid fuels such as coal.



140 Vista-LA also includes two additional sources that are not explicitly accounted for in the California GHG
141 Inventory but are potentially significant sources of fugitive CH₄ emissions in SoCAB: compressed natural
142 gas (CNG) fueling stations and liquefied natural gas (LNG) fueling stations, which were categorized
143 under IPCC Level 2 – 1B2. This case study of Vista-LA focuses on anthropogenic sources of CH₄, and
144 every effort has been taken to make the Vista-LA dataset as complete, accurate, and timely as possible.
145 Because Vista-LA is designed to incorporate solely anthropogenic sources of CH₄, natural CH₄ sources
146 such as wetlands and geologic seeps are excluded this version. This is consistent with the most recent
147 version of the California GHG Inventory, which categorizes petroleum gas seeps separately as “excluded”
148 emissions, though they were previously categorized under IPCC – 1B2.

149 **2.2 Overview of Data Sources**

150 Within each of the three major CH₄ source sectors (IPCC 1 - Energy, IPCC 3 - Agriculture, Forestry, and
151 other Land Use; and IPCC 4 - Waste), we defined the types of infrastructure associated with emissions.
152 We sought out publicly available datasets that mapped their spatial locations (Table 1). Spatial datasets
153 were compiled from reliable and verified public databases on government and federal/state research
154 agency portals. The data are presented as shapefiles and kmz files that include point, line, and polygon
155 data. Table 1 summarizes the spatial datasets by the year, source of data, data type (points, lines, or
156 polygon data) and also indicates the corresponding IPCC Level 3 CH₄ emissions category. Sections 3-5
157 describe the data sources and information in Vista-LA in further detail and also describe the specific data
158 processing techniques applied to the GIS dataset for each of the Level 3 emissions category.

159 Some of the spatial datasets we obtained (see e.g., Southern California Association of Governments,
160 <http://gisdata.scag.ca.gov/Pages/GIS-Library.aspx>) and EPA Facility Registry Service (FRS) were useful
161 for evaluating information from more than one type of CH₄-producing infrastructure (e.g., petroleum
162 refineries and wastewater treatment plants). Due to the variety of data sources used to create Vista-LA,
163 the same level of detail (e.g., spatial resolution, data completeness, available metadata) was not always
164 available for every CH₄ emitting source. The level of completeness or detail for each spatial dataset will
165 be discussed below under the data sources and limitations sections. We processed and standardized GIS



166 datasets through geo-referencing, spatial configuration, and verification using ArcGIS software packages.
167 All spatial features and raster layers were geo-located using the World Geodetic System 1984 datum and
168 the Universal Transverse Mercator Zone 11 North coordinate system. Considerations for privacy
169 including restrictions and limitations on some of these datasets were taken into account for the final
170 product. Consequently, Vista-LA datasets for natural gas compressor stations and natural gas pipelines
171 are only included as static representations in Figures 2 and 3. Vista-LA does not include sub-facility level
172 information. Timely data are critical for understanding methane dynamics in SoCAB, therefore we used
173 the most current publicly available information in the development of the Vista-LA database.

174 **3 Energy (IPCC Level 1 – Category 1)**

175 The Energy (IPCC Level 1 – 1) sector includes CH₄ emitted by fuel combustion activities (IPCC Level 2
176 – 1A) and fugitive emissions from fuels (IPCC Level 2 – 1B). CH₄ emissions from fuel combustion are
177 mainly produced by energy industries and transportation, with minor contributions from manufacturing,
178 commercial, industrial, residential and agricultural fuel combustion (CARB, 2016). Fugitive emissions
179 are defined by the IPCC as an intentional or unintentional release of gas from anthropogenic activities not
180 including combustion (IPCC, 2001). Fugitive CH₄ emissions come from leaks or failures of equipment,
181 off-gassing, or venting, arising from sources such as natural gas storage facilities, oil and gas wells, and
182 pipelines. They occur mainly in the oil and gas sector (~95% of California’s estimated fugitive CH₄
183 according to CARB, 2016), with a small contribution from industrial and manufacturing sources. Many
184 facilities, including petroleum refineries and power plants, include both combustion and fugitive CH₄
185 emissions.

186 **3.1 Fuel Combustion Activities (IPCC Level 2 - 1A)**

187 Fuel combustion activities (IPCC Category 1A) includes CH₄ emissions from energy industries, which
188 encompass petroleum refining and electricity generation via combustion of natural gas in power plants,
189 and transportation. Other combustion sources have only a small expected CH₄ emission rate (totaling
190 <0.1% of statewide CH₄), according to the California GHG Inventory, hence are not included in Vista-
191 LA (CARB, 2016). The physical infrastructure associated with combustion and fugitive CH₄ emissions



192 from energy industries in SoCAB are natural gas-fired power plants and petroleum refineries.
193 Transportation comprises ~1.1% of inventoried statewide CH₄, primarily from on-road sources (e.g.,
194 conventionally fueled cars, light- and heavy-duty trucks), but is not included in this version of Vista-LA
195 (CARB, 2016).

196 **3.1.1 Energy Industries (IPCC Level 3 - 1A1)**

197 **3.1.1.1 Petroleum Refineries (Vista-LA layer)**

198 *Data sources:*

199 The Vista-LA petroleum refinery dataset provides location and extent data for 12 facilities in the domain.
200 The primary spatial datasets for petroleum refineries (IPCC – 1A1) were gathered from the U.S. Energy
201 Information Administration (EIA) for the year 2016. EIA reports information about all operable
202 petroleum refineries and electricity generation plants in the United States, including plants that are active,
203 on standby, and those short-term or long-term out of service (EIA, 2016). Additional information came
204 from Southern California Association of Governments (SCAG) land use data for the years 2005 and 2012
205 (see <http://gisdata.scag.ca.gov/Pages/GIS-Library.aspx>).

206 *Data processing and validation:*

207 Petroleum refinery locations were verified using multiple datasets, including EIA, SCAG, and the ESRI
208 Basemap aerial imagery, and Google Earth imagery. EIA was the primary source of information, as it
209 contains the most recent data. SCAG was used to verify that there were no missing petroleum refineries
210 from EIA. This process provided data quality assurance from the most updated publicly available spatial
211 database of petroleum refineries.

212 The original EIA data series on petroleum refineries includes geolocations as points, and information on
213 production capacity, current and projected capacity of crude oil separated by atmospheric distillation,
214 downstream charge, as well as fuel, electricity, and steam purchased and consumed by 141 refineries



215 across the United States (U.S. Energy Information Administration, 2015). This dataset contains
216 information on nine refineries located in SoCAB, all of which are located in Los Angeles County.

217 To map the area of petroleum refinery and power plant facilities, we added data from SCAG for the years
218 2005 and 2012, which maps land use areas to a minimum two acre resolution (see
219 <http://gisdata.scag.ca.gov/Pages/GIS-Library.aspx>). The SCAG database only contains land use
220 classifications for the State of California, and lacks facility-level information. We performed feature
221 identification using SCAG land use code 1322 “Petroleum Refining and Processing”. This category
222 includes major oil refineries, as well as associated petrochemical plants. This data was used to identify,
223 extract, and define the spatial extent of each refinery and match the geolocations of the refineries listed
224 in the EIA 2016 dataset.

225 The SCAG land use code was used to identify and extract 30 polygons in the SCAG 2005 dataset and 60
226 polygons in the SCAG 2012 dataset related to petroleum refineries in SoCAB. Because SCAG polygon
227 features were fragmented and not assigned to an individual refinery, they had to be manually merged
228 based on their geolocation and spatial relation to the EIA 2016 dataset. The polygon features dataset
229 categorized as “Petroleum Refining and Processing” were merged together and then compared to the nine
230 refineries identified in the raw EIA dataset. In some cases, these SCAG polygon features were
231 geographically misplaced in residential locations or in the middle of streets and had to be manually
232 adjusted to fit the actual extent of that facility. There were three facilities identified in the SCAG dataset
233 that were not identified in the EIA dataset. The existence and operation of these three facilities identified
234 in SCAG were further verified using refinery planning documents and environmental assessment reports
235 and then were appended to the EIA dataset. The true spatial extent of all polygons was verified using
236 aerial imagery. During validation of refinery spatial extents with Google Earth Imagery and Esri Basemap
237 aerial imagery, focus was given on identifying acres of storage tanks situated in a matrix formation, large
238 intake pipes, storage vats, and large industrial infrastructure.

239 *Limitations:*



240 The additional refineries identified in SCAG and validated through the Vista verification procedures do
241 not contain facility level metrics that were provided in the EIA dataset. Obtaining detailed sub-facility-
242 level information for each petroleum refinery will be crucial to developing accurate CH₄ emission factor
243 estimates.

244 *Results:*

245 The final Vista-LA petroleum refinery dataset includes all 12 petroleum refineries operated by eight
246 different companies within SoCAB. The final dataset includes operational data from EIA, recalculated
247 locational data, and validation notes including any changes made and date of last update.

248 **3.1.1.2 Power Plants (Vista-LA layer)**

249 *Data sources:*

250 The Vista-LA layer for power plants (IPCC – 1A1) relies on data from EIA, SCAG 2005, SCAG 2012,
251 Google Earth and Esri Basemap aerial imagery (EIA, 2016; see <http://gisdata.scag.ca.gov/Pages/GIS-Library.aspx>). The Vista-LA power plant dataset provides accurate location and extent data as well as
252 facility level information on the type of power generation methods and energy production statistics.
253

254 *Data processing, validation and limitations:*

255 The EIA 2016 contains records for 7,995 power plants in the United States, including 385 power plants
256 in SoCAB. For our analysis, we selected only the power plants that used the following primary fuels:
257 biomass, natural gas, petroleum, or other—which matches the methods of the California GHG inventory
258 (CARB, 2016). This excluded power plants with primary fuel categories such as wind, solar,
259 hydroelectric, or pumped storage. After filtering by primary fuel type, the new dataset contained 110
260 power plants in SoCAB.

261 Polygon features for each of the 110 power plants were created based on Google Earth Imagery, Esri
262 Basemap Aerial Imagery, SCAG 2005 and SCAG 2012 land use datasets. The SCAG land use code 1431



263 (“Electrical Power Facilities”), was used to verify and determine the spatial extent of the EIA power
264 plants. SCAG polygons were geolocated with the point data from the EIA dataset. In total, there were
265 1,490 individual polygon features related to land use code 1431 in SCAG 2005 and 6,932 in SCAG 2012.
266 In addition to power plants, the SCAG land use code 1431 also includes land used for distribution of
267 electricity and substations with power plants, hence visual inspection using high-resolution aerial imagery
268 was required to validate each individual power plant and to generate accurate polygon representations.

269 When visually inspecting individual power plants, we looked for typical power plant infrastructure
270 features such as smoke or steam stacks with towers, racks, piping, and vents, transformers and/or electrical
271 equipment. Some power plant locations were more difficult to validate. In some cases, the power plant
272 point data was placed on the street near the operating utility and sometimes it did not match the address
273 that was listed in the metadata. Sometimes the point was located on the center of a site, which could be
274 within another facility (e.g. a refinery) and thus had to be manually adjusted with appropriate
275 understanding of the context of its location using Google Earth and Esri Basemap aerial imagery.
276 Polygons were created using GIS methods including geoprocessing and digitizing with Google Earth and
277 Esri Basemap aerial imagery as reference. Power plant latitude and longitude coordinates were
278 recalculated appropriately for each power plant. Power plants whose geolocations were verified but their
279 spatial extents could not be determined using this method were tagged with a circular placeholder and
280 their EIA facility level metrics were maintained and marked in the metadata.

281 We used the 2014 Fossil Fuel Data Assimilation System (FFDAS) point dataset to validate our results
282 (Asefi-Najafabady et al., 2014). The 105 power plant point locations in the 2014 FFDAS dataset match
283 with 105/110 power plants in the final Vista-LA layer. The FFDAS dataset includes only those facilities
284 registered through CAMD and EIA reporting, which explains the difference in the number of locations
285 between the two datasets. One of the five plants is a landfill gas plant, so it is not tracked in FFDAS
286 because it is not a fossil-based source of CO₂ emissions.

287 We also considered using the 2010 Open-source Data Inventory for Anthropogenic CO₂ (ODIAC) for
288 validation of power plants (Oda and Maksyutov, 2011). Cross-validation with ODIAC was not
289 straightforward because the online data product is gridded and is at lower resolution than the EIA and



290 SCAG datasets. The publicly available version of ODIAC also had significant latency compared to the
291 EIA and SCAG datasets used in this study.

292 *Results:*

293 The Vista-LA power plant dataset merged polygon extent data with the EIA metadata. The final dataset
294 includes the facility level statistics from EIA and along with data validation information using Google
295 Earth, SCAG 2005, and SCAG 2012 in the metadata for all 110 power plants originally identified in the
296 EIA dataset. Based on the 2016 EIA electrical output data, there are only 17 power plants with greater
297 than 100 Megawatts/hour of electrical output in SoCAB. For this reason, we include the production
298 metrics in the Vista-LA database, as they may be useful for generating CH₄ emission estimates in the
299 future. The largest producing power plants in SoCAB might be expected to have significant emissions of
300 CH₄ compared to smaller power plants.

301 **3.2 Fugitive Emissions from Fuels (IPCC Level 2 - 1B)**

302 Fugitive emissions from fuels (IPCC Category 1B) include CH₄ emissions from the lifecycle (production,
303 processing, storage, transportation) of oil, natural gas, solid fuels, and geothermal energy production
304 occurring in SoCAB. We omit the latter two sources from consideration since California air quality
305 restrictions do not permit coal-burning (Perata, 2006), and there are no active coal mining or geothermal
306 energy sites in the SoCAB. In the California GHG inventory, fugitive emissions are primarily from oil
307 and gas extraction (30%) and natural gas pipelines (65%) (CARB, 2016). Vista-LA includes spatial
308 information for oil & gas wells, natural gas pipelines, natural gas storage fields, natural gas processing
309 plants, and natural gas compressor stations. Petroleum refineries emit fugitive CH₄ (IPCC 1B2), but
310 because of the spatial overlap with refinery combustion emissions at the facility level, we do not treat
311 them separately in Vista-LA (see refinery layer in IPCC Category 1A1). We also include two more
312 potentially significant sources of fugitive CH₄ emissions in SoCAB that have no assignment in the
313 California GHG inventory or IPCC categories: compressed natural gas (CNG) fueling stations and
314 liquefied natural gas (LNG) fueling stations. Vista-LA does not yet include the locations of petroleum
315 storage tanks due to a lack of publicly available information for these elements. Data for energy-related



316 sources is also available for purchase from consulting companies; however, one of the objectives of this
317 work is to generate a product that is openly accessible to the public. Therefore, we did not utilize
318 proprietary or “for-purchase” information in the development of the Vista-LA database.

319 **3.2.1 Oil and Natural Gas (IPCC Level 3 - 1B2)**

320 **3.2.1.1 Compressed Natural Gas (CNG) Fueling Stations (Vista-LA layer)**

321 *Data sources:*

322 Geospatial data of active compressed natural gas (CNG) fueling stations was obtained from the U.S.
323 Department of Energy’s (DOE) Alternative Fuels Data Center (AFDC) for the year 2017 (DOE, 2017).
324 Currently, CNG fueling stations are not included in a separate IPCC category, so for the purposes of this
325 study we have classified these data under IPCC Level 3 – 1B2)

326 *Data processing, validation and limitations:*

327 The raw file was downloaded from DOE/AFDC through a series of queries for compressed natural gas
328 stations. Next, the CNG dataset was geocoded using latitude/longitude coordinates. Coordinates for this
329 dataset generated points for 1,792 stations across the United States including 336 in the state of California.
330 163 of the 336 compressed natural gas stations were in SoCAB, further reduced to 109 after removing
331 duplicate entries. The geolocations of these 109 CNG fueling stations were verified by comparing the
332 reported street address to Google aerial imagery (e.g. Google Earth, Google Maps, and Google Earth
333 Street View) and Esri Basemaps. Out of the 109 points, 88 polygon extent features were created based on
334 aerial imagery. For the remaining 21 CNG stations, placeholder polygons were created for stations whose
335 natural gas infrastructure could not be visually identified using aerial imagery, but whose location was
336 otherwise verified. During visual validation of the CNG stations, we focused on identifying pumps, gas
337 station infrastructure, and piping/compressed gas storage cylinders near parking lots and salvage yards.

338 A major portion of the DOE/AFDC dataset placed the locations of CNG fueling stations adjacent to the
339 fueling station, making it challenging to discern the exact location of station infrastructure on the map.



340 This dataset counts the entire station as one polygon, despite multiple fuel dispensers. Sub-facility-level
341 information about individual fueling dispensers is not currently identified in Vista-LA.

342 *Results:*

343 The final Vista CNG station layer contains geolocations for 109 polygons. The metadata contains
344 information about the station name, pressures (units: pounds per square inch or psi), types of dispensing
345 capability, maximum vehicle size accommodation, and the recalculated latitude and longitude
346 coordinates, along with validation notes including any changes made and date of last update.

347 **3.2.1.2 Liquefied Natural Gas (LNG) Fueling Stations (Vista-LA layer)**

348 *Data sources:*

349 Similar to CNG stations, fugitive emissions from LNG fueling stations were not inventoried in the 2015
350 California GHG Inventory. Thus, we assigned LNG stations under IPCC – 1B2. Geospatial data of active
351 LNG fueling stations was obtained from the U.S. Department of Energy’s (DOE) Alternative Fuels Data
352 Center for the year 2017 (DOE, 2017).

353 *Data processing, validation and limitations:*

354 DOE data was originally geocoded using the coordinates listed. The raw DOE dataset contained 187
355 records of LNG stations across the U.S., 47 of those stations were located in the state of California with
356 27 currently open and operational in SoCAB. 15 of the 27 LNG stations shared the same location with
357 CNG stations. The geolocations of the 12 LNG-only stations were verified by comparing the reported
358 street address to Google aerial imagery and Esri Basemap aerial imagery. Similar to the CNG stations,
359 extent polygons were generated of the remaining 12 stations using aerial imagery. During visual
360 validation of the LNG stations, focus was given on identifying gas station infrastructure, and
361 piping/compressed gas storage cylinders near parking lots and salvage yards.



362 This dataset is updated annually by the DOE, meaning additional validation will need to be completed in
363 the future as more LNG fueling stations come online. Two stations were already listed as being planned
364 in SoCAB and will be operational in less than a year and will need to be added to the dataset in the future.
365 Similar to the CNG dataset, the LNG dataset assigns the entire station as one polygon, regardless of the
366 number of fuel dispensers.

367 *Results:*

368 The final Vista-LA LNG fueling stations dataset contains polygons for 27 stations in SoCAB. The LNG
369 dataset also includes metadata describing the station name, pressures (units: psi), types of dispensing
370 capability, maximum vehicle size accommodation, recalculated GPS coordinates, and validation notes
371 including any changes made and date of last update.

372 **3.2.1.3 Natural Gas Compressor Stations (Vista-LA layer)**

373 The natural gas compressor station (IPCC – 1B2) dataset was obtained using the U.S. Environmental
374 Protection Agency’s Facility Level Information on GHG online reporting Tool (EPA FLIGHT). We
375 approximated their locations of non-reporting facilities using the EIA compressor station database, which
376 provides postal-code-level information on compressor stations (Maasakkers et al., 2016). We identified
377 two natural gas compressor stations in SoCAB. The locations of both natural gas compressor stations
378 were validated using Google Earth and Esri Basemap aerial imagery (EPA, 2015). Due to restrictions, we
379 only show the location of the reporting compressor station facility in Figures 2 and 3. The EPA data can
380 be complemented with the EIA database for non-reporting facilities for potential future development of
381 gridded emissions products.

382 **3.2.1.4 Natural Gas Pipelines (Vista-LA layer)**

383 Information for natural gas pipelines (IPCC – 1B2) was collected from the California Energy Commission
384 (CEC) and the EIA 2017 dataset (Maasakkers et al., 2016). The CEC dataset provides infrastructure
385 information of major gas transmission and hazardous liquid transmission pipelines in the United States
386 for the year 2012 (CEC, 2012). For California, the raw CEC dataset was georeferenced and clipped to fit



387 the spatial extent of SoCAB. We also obtained high-resolution natural gas transmission pipeline maps
388 from the National Pipeline Mapping System (NPMS) to validate the CEC pipeline layers. The NPMS
389 dataset includes a level of detail similar to that of the CEC dataset, but can be obtained for the entire U.S.
390 There were very minor differences between the CEC and NPMS layers; However, because the NPMS
391 restricts distribution or visualization of this data, they were retained for internal use only. Due to security
392 concerns, the CEC dataset is only shown as static representations in Figures 2 & 3.

393 Unlike the CEC and NPMS data, the EIA dataset is available publicly. The EIA dataset has a lower level
394 of accuracy compared to the CEC dataset. The positional accuracy of the EIA dataset is $\pm 3,000$ meters
395 while the positional accuracy of CEC ± 150 meters. The EIA dataset also contains less information on the
396 disaggregation of pipeline segments. The final Vista-LA natural gas pipeline dataset includes a
397 georeferenced and processed version of the EIA dataset and contains 111 polyline segments, however due
398 to the uncertainties noted, it would be ideal to use more spatially resolved datasets for future work.

399 **3.2.1.6 Natural Gas Storage Fields (Vista-LA layer)**

400 *Data sources:*

401 Under IPCC – 1B2, natural gas storage facility point data for the United States was obtained from the
402 U.S. Energy Information Administration (EIA) online database for 2016 (EIA, 2016). Natural gas storage
403 geolocations and spatial extent data were obtained using oil field extents from California Department of
404 Conservation’s Division of Oil, Gas, & Geothermal Resources (DOGGR) for 2016 (DOGGR, 2016). The
405 EPA FLIGHT tool was also used for data quality assurance (EPA, 2015).

406 *Data processing, validation and limitations:*

407 Point locations for natural gas storage from EIA in 2016 included 415 points for the entire United States,
408 three of which are in SoCAB. Since underground natural gas storage in California is done in depleted oil
409 fields (EIA, 2008), we determined natural gas storage field extents using the 2016 DOGGR dataset, which
410 contained 516 polygon features for oil field extents in the state of California. Both datasets were first
411 georeferenced. The EIA metadata contained operation metrics for each storage field, which we appended



412 to the DOGGR polygon shapefiles for these three extracted entries. The EPA FLIGHT online GHG
413 reporting tool was used to validate the geolocations of the Aliso Canyon and Honor Rancho storage
414 facilities. Southern California Gas Company's online information on natural gas storage facilities
415 validated the geolocation and extent of the Playa Del Rey storage facility.

416 We did not include former gas storage fields that are no longer used, such as the Montebello Oilfield.
417 Nevertheless, it is possible these former storage facilities are still leaking, as it takes many years to deplete
418 the gas to pre-storage conditions (Chilingar and Endres, 2005).

419 *Results:*

420 The Vista-LA natural gas storage field polygon layer contains the spatial information and attribute
421 information of the three natural gas storage facilities located within SoCAB: Aliso Canyon, Honor
422 Rancho, and Playa Del Rey. The final Vista-LA layer contains metadata relating to field type, company
423 name, amount of base gas, working capacity, field capacity, maximum delivery, and recalculated
424 locational coordinates along with validation notes including any changes made and date of last update.

425 **3.2.1.5 Natural Gas Processing Plants (Vista-LA layer)**

426 *Data sources:*

427 Natural gas processing plant (IPCC 1B2) geospatial data was obtained from the U.S. Energy Information
428 Administration (EIA) online database for the year 2014 (EIA, 2016).

429 *Data processing, validation and limitations:*

430 The raw 2014 EIA dataset contained point geolocations for 551 processing plants across the United States,
431 with six of these in SoCAB, which were georeferenced. Because the raw EIA dataset was limited to a
432 scale of 1:1,000,000, extensive manual geolocation and validation had to be completed for each plant.
433 EIA's geolocation was manually augmented using aerial imagery, planning documents and environmental
434 assessment reports related to the operating companies of each processing plant. Exact spatial extents for



435 the processing plants were created by identifying infrastructure features such as electrical equipment,
436 piping, vents, smoke or steam stacks with towers, racks, and transformers using both Google Earth and
437 Esri Basemap imagery.

438 *Results:*

439 The Vista-LA natural gas processing plant layer contains verified geolocated polygons of six facilities
440 located in SoCAB. The associated metadata includes information on facility and operator name, plant
441 flow in million cubic feet per day, dry storage in million metric standard cubic feet, energy content of
442 natural gas in British thermal units, barrels of liquid natural gas stored at each facility, recalculated
443 locational coordinates of each polygon, along with validation notes including any changes made and date
444 of last update.

445 **3.2.1.7 Oil and Gas Wells (Vista-LA Layer)**

446 *Data sources:*

447 Data on oil and gas wells was collected from DOGGR for the year 2016 (DOGGR, 2016). The oil and
448 gas well dataset contains information on well status, type, coordinates, and whether it has undergone
449 hydraulic stimulation treatment. Another dataset from DOGGR also includes historical production and
450 injection statistics, owner and operators of the well, and the state of the well.

451 *Data processing, validation and limitations:*

452 In SoCAB, the DOGGR dataset includes 32,537 oil and gas wells, associated with activities such as gas
453 storage, pressure maintenance, water disposal, and other (DOGGR, 2016). Due to the sheer size of the
454 datasets, we assumed the locations of the wells in the DOGGR dataset to be valid for the purposes of this
455 study. The dataset includes 5,804 abandoned wells, some of which may be located underneath buildings
456 and other structures which hinder validation of their locations (Chilingar and Endres, 2005). Validation
457 of this dataset is beyond the scope of this work, even in cases where manual visual inspection methods



458 and/or automated feature extraction from aerial imagery might be useful. We discuss possible methods
459 for automated feature extraction using aerial imagery further in Section 6.

460 According to DOGGR, well information varies in accuracy, scale, origin and completeness (DOGGR,
461 2016). DOGGR uses a variety of sources to establish well locations. These sources include handheld
462 measurements using GPS units derived from DOGGR Division staff, coordinates provided by operators,
463 well summary reports, official notices regarding the intent to drill, coordinates derived from aerial
464 imagery, coordinates generated from a tool in MapInfo based on corner call locations, and coordinates
465 from digitized maps. However, we note that some wells in LA were drilled before accurate records were
466 kept by DOGGR (Chilingar and Endres, 2005).

467 **4 Agriculture, Forestry, and Other Land Use (IPCC Level 1 - Category 3)**

468 In the California GHG Inventory, emissions from Livestock (IPCC Category 3A) are the largest of the
469 IPCC Level 3 categories (Figure 1). Emissions from Biomass Burning (IPCC – 3C1) contribute at the
470 ~0.1% level (Figure 1), and are therefore considered negligible for the purposes of this study. Emissions
471 from Wetlands (IPCC – 3B4) and all other emissions from the Land (IPCC Category 3B), Aggregate
472 Sources and Non-CO₂ Emissions (IPCC Category 3C) and Other (3D) source types of the Agriculture,
473 Forestry and Other Land Use category are also considered insignificant in the domain, and were not
474 included as part of this study. Within the Livestock category, dairies and cattle farms are the major
475 contributors in the SoCAB region (Viatte et al., 2017). Below we describe our methods for collecting GIS
476 data related to these activities within the SoCAB.

477 **4.1 Livestock (IPCC Level 2 - 3A)**

478 The livestock category (IPCC – 3A) includes emissions from enteric fermentation (IPCC – 3A1) and
479 manure management (IPCC – 3A2). Manure management systems vary from facility to facility and
480 broadly fall into dry and wet management practices (Kaffka et al., 2016). Manure can be handled and
481 stored using dry lots, deep pits, solid manure storage, daily spread, digesters (CARB, 2016). In
482 slurry/liquid systems, waste from feedlots and other livestock areas are washed and is collected in ponds,
483 which are commonly referred to as anaerobic lagoons (Kaffka et al., 2016). Emissions from manure



484 depend the type of management practices employed by the farm or facility (Kaffka et al., 2016). Wet
485 manure management involves washing of feedlots and other livestock areas, and the waste runoff is
486 typically collected in lagoons where CH₄ is produced due to anaerobic conditions. By contrast, dry manure
487 management practices do not wash waste with water, thus reduce anaerobic conditions. Dairies in SoCAB
488 primarily use dry manure management practices due to the copious amounts of water needed in wet
489 manure management practices for the collection, movement and storage of animal wastes. However,
490 recent mobile measurement campaigns verified CH₄ emissions from a small number of dairies with
491 anaerobic lagoons as recently as 2015 (Hopkins et al., 2016b; Viatte et al., 2017). In addition to dairy
492 locations, the locations of some anaerobic lagoons were identified as part of the Vista-LA database as
493 described below.

494 **4.1.1 Enteric Fermentation (IPCC Level 3 - 3A1)**

495 **4.1.1.1 Dairies (Vista-LA Layer)**

496 *Data sources:*

497 Dairy and cattle farm facility data were collected from the California Regional Water Quality Control
498 Board (RWQCB), Santa Ana Region. The data was drawn from annual reports, which contain information
499 on the location of each dairy, the number and type of the herd (i.e., milking cow, dry cow, heifer or calf)
500 and other livestock located at each facility for the year 2015 (Kashak, 2016). We defined cattle farms as
501 facilities that did not contain any milking cows. Overall, dairy facilities were primarily found to be
502 located in the Chino and in the San Jacinto Basins.

503 *Data processing, validation and limitations:*

504 First, the raw RWQCB dataset was georeferenced to match the spatial information of the datasets in Vista-
505 LA. Next, all 110 locations of dairies and cattle farms were validated with Google Earth's historical
506 imagery tool for the year 2015. Facility addresses and coordinates were used to validate the true locations
507 of the farms. When verifying with aerial imagery, focus was given to dairy/cattle facility infrastructure
508 such as: feedlots, manure lagoons, animal housing structures, and open pastures. The dairy and cattle farm



509 locations were deemed accurate if the geographic location in the RWQCB dataset was confirmed with
510 aerial imagery and the coordinates did not overlap another facility. During processing and validation, we
511 identified and manually corrected the locations for two farms with incorrect addresses based on aerial
512 imagery. Additionally, we corrected geolocations for twelve farms that were located incorrectly in the
513 original RWQCB dataset using Google Earth aerial imagery and the facility address information given in
514 the RWQCB dataset.

515 The RWQCB did not report the quantity of feedlots or manure lagoons per dairy, but did include several
516 other types of information which will be useful for estimating emissions from manure management,
517 including: annual manure produced, manure hauled, manure spread to cropland and amount of wastewater
518 produced. The RWQCB dataset also contained several facilities that were neither dairy nor cattle farm,
519 such as a livestock market and beef packing facilities. We removed these from the final Vista-LA layer
520 because we do not expect significant CH₄ emissions from these facilities.

521 It was difficult to obtain spatial extent for each facility because they were difficult to differentiate, as
522 many facilities displayed common features. For this reason, all final dairy/cattle facility locations are
523 point-based in the Vista-LA database. The RWQCB database did not report the number of milking cows,
524 dry cows, heifers or calves for the seven of the farms in Chino. While it does not affect the geolocation
525 in our facility maps, information on cattle populations specific to these farms will be helpful for estimating
526 CH₄ emissions from these facilities.

527 *Results:*

528 The final Vista-LA dairy layer contains a total of 110 livestock facilities in SoCAB: 22 dairies and one
529 cattle farm in the San Jacinto Basin; and 56 dairies, 26 cattle farms and five other livestock farms in
530 Chino. Locations for all facilities were validated using Google Earth imagery. Validation notes have been
531 appended to the spatial dataset for further information on which facilities were corrected for location.



532 **4.1.2 Manure Management (IPCC Level 3 - 3A2)**

533 **4.1.2.1 Anaerobic lagoons (Vista-LA layer)**

534 *Data sources:*

535 In terms of manure management practices, Vista-LA focused on the collection of GIS structures for wet
536 manure management. Specifically, anaerobic lagoons (IPCC – 3A2) were identified using visual
537 inspection of aerial imagery since publicly available GIS datasets on anaerobic lagoons were not
538 available. Therefore, we created a preliminary geospatial dataset of SoCAB anaerobic lagoons starting
539 from the dairies and cattle farms GIS data. Anaerobic lagoons, also commonly called manure lagoons,
540 are considered sub-facility infrastructures within dairy/cattle farms.

541 *Data processing, validation and limitations:*

542 Point locations of manure lagoons at each dairy farm were visually determined using aerial imagery from
543 the National Agriculture Imagery Program (NAIP) and Google Earth's Time Tool for the year 2015.
544 Infrastructure of anaerobic lagoons were identified near a dairy/cattle farm facility by their distinct
545 rectangular shape and brown to dark blue color associated with the color of wash water from manure
546 waste. Often, aerial imagery showed evidence of cattle, further confirming the facility location. Once a
547 lagoon structure was identified, GIS processing tools were used to create point data for the geolocation.

548 Most anaerobic lagoons in SoCAB were found in the Chino/Ontario region, the area with the densest
549 clusters of dairy farms. However, the identified geolocation of lagoons for year 2015 is likely to change
550 in the near future due to rapid land use developments in the region and fluctuating manure management
551 practices (Hirsch, 2006). Further work could be done with automated feature extraction with
552 contemporaneous imagery, as discussed in Section 6.3.

553 *Results*



554 The Vista-LA layer for anaerobic lagoons contains 228 point locations in the Chino, Ontario, and
555 Riverside regions. The final layer includes geolocations given by latitude and longitude with validation
556 notes including any changes made and date of last update.

557 **5 Waste (IPCC Level 1 – Category 4)**

558 **5.1 Solid Waste Disposal (IPCC Level 2 - 4A)**

559 Solid waste disposal includes both managed and unmanaged waste disposal sites, as well as uncategorized
560 disposal sites. The largest CH₄ emissions are expected from managed waste disposal sites, hence the site
561 category we included in the Vista-LA data product.

562 **5.1.1 Managed Waste Disposal (IPCC Level 3 - 4A1)**

563 Managed Waste Disposal (IPCC – 4A1) is the third largest IPCC Level 3 emissions source in the
564 California GHG inventory, trailing only the Enteric Fermentation (IPCC – 3A1) and Manure Management
565 (IPCC – 3A2) categories. Landfills (solid waste disposal sites) constitute the source of Vista-LA data for
566 this source. Vista-LA includes both active and inactive landfills, with the status recorded in the metadata.

567 **5.1.1.1 Landfills (Vista-LA Layer)**

568 *Data sources:*

569 The Vista-LA layer for landfills (IPCC – 4A1) was created using the California Air Resource Board's
570 2014 landfill data and the 2015 California's Department of Resources Recycling and Recovery's
571 (CalRecycle) Solid Waste Information System (SWIS) dataset (CARB, 2014; CalRecycle, 2015).
572 Geolocation and spatial extent for each individual landfill facility was generated and verified using the
573 2005 and the 2012 SCAG land use dataset, Google Earth, and Esri Basemap aerial imagery (see
574 <http://gisdata.scag.ca.gov/Pages/GIS-Library.aspx>).

575 *Data processing, validation and limitations:*



576 The CARB 2014 landfill dataset contained locational records for 372 potential methane-producing
577 landfills for the state of California with 73 of those landfills located in SoCAB. The CalRecycle/SWIS
578 point dataset contained information on 3,087 landfills for all of California, with 759 in SoCAB.
579 CalRecycle landfills located in SoCAB were queried to isolate only the 353 tagged as “solid waste
580 disposal facilities” or “solid waste landfills”. Finally, 19 duplicate entries were identified and removed.

581 The geolocation and spatial extent of the 334 unique landfills in the CalRecycle/SWIS dataset were
582 verified using SCAG 2005 and SCAG 2012 land use datasets. We used the SCAG land use code 1432
583 (solid waste disposal facilities) to identify the polygon features associated with active dumps and sanitary
584 landfill operations. We used both SCAG 2005 and SCAG 2012 for maximum amount of information on
585 landfill extent information because neither SCAG dataset contained all landfill locations. In the raw
586 SCAG 2005 dataset, there were 247 individual polygons associated with the land use code 1432 in
587 SoCAB. The SCAG 2005 dataset showed multiple polygon features for the same facility in some cases,
588 so this dataset was further refined by merging multiple polygons that comprise a known facility location
589 based on the refined CalRecycle/SWIS dataset. Simplified polygon features were created for all the
590 distinguishable solid waste disposal sites based on cross-checking the SCAG dataset with the point data
591 from CalRecycle and World Imagery. In Los Angeles County, the 86 total polygons associated with land
592 use code 1432 were aggregated into 18 individual landfills; in Orange County, 60 polygons were
593 aggregated into 7 individual landfills; in Riverside County, 61 polygons were aggregated into 13
594 individual landfills; and in San Bernardino County, 40 polygons were aggregated into 10 individual
595 landfills. This process was again repeated using the SCAG 2012 dataset that had 211 polygons designated
596 as land use code 1432. Overall, 48 landfills of the total 334 were identified from the intersection of SCAG
597 2005/2012 solid waste disposal facilities and landfills from the CalRecycle/SWIS dataset.

598 The location and spatial extent of the remaining 286 landfills from the CalRecycle/SWIS dataset had to
599 be manually validated and/or generated using Google Earth Imagery along with other GIS methods
600 including geoprocessing and digitizing. We were able to verify the location of 188 out of the 286
601 designated landfills. Unfortunately, their extent and shape could not be determined using imagery since
602 they had long been closed and thus modified or built upon significantly. A placeholder polygon was



603 generated indicating the historical location with extent and shape determined and digitized using Google
604 Earth imagery (for example canyons, excavated pits, and barren land). However, land use changes that
605 occur on surfaces of former landfills vary from site to site. As seen with verification procedures for power
606 plants, time sensitive imagery is critical when evaluating the existence and geolocations of landfills. Using
607 the CalRecycle/SWIS metadata for address location for enhanced verification proved to be difficult
608 because often there were no landfill related features at these addresses, requiring manual geolocation and
609 correction.

610 The verified 334 polygons were subset by matching the SWIS number in the CalRecycle metadata to the
611 SWIS number of the 73 potential methane-producing landfills in the CARB dataset in order to produce
612 the final Vista-LA dataset.

613 *Results:*

614 In total, 73 potential methane-producing landfills were identified, all locations verified, and polygons
615 were generated in the final dataset using the actual extent or placeholder if extent could not be verified.
616 The metadata from the CalRecycle/SWIS dataset was appended to the final Vista-LA landfill polygon
617 dataset. This includes site-specific information, such as throughput, capacity, and waste types
618 (CalRecycle, 2015). Validation notes include whether facility extent was derived from SCAG 2005,
619 SCAG 2012, or Google Earth imagery. The final polygon data for landfill extents can be separately
620 categorized by landfill status: active, closed, clean-closed, closing, absorbed, and inactive. The operation
621 status breakdown is as follows: 2 were absorbed, 17 were active, 3 were clean-closed (site is considered
622 to cease to exist as a solid waste disposal site, but records are kept to document the status of the site), 308
623 were closed, 1 was closing, and 3 were inactive.

624 **5.2 Wastewater Treatment and Discharge (IPCC Level 2 – 4D)**

625 Wastewater treatment and discharge includes both domestic and industrial wastewater treatment facilities
626 (Table 1).



627 **5.2.1 Domestic and Industrial Wastewater Treatment and Discharge (IPCC Level 3 – 4D1 and 4D2)**

628 Wastewater treatment in SoCAB is primarily done through aerobic sludge digestion, which has no
629 associated CH₄ emissions in the California GHG inventory (CARB, 2016). However, in low oxygen
630 conditions, CH₄ may be emitted as a by-product of enhanced denitrification present in water recycling
631 systems (e.g., open tanks in treatment facilities; Townsend-Small et al., 2012). Many wastewater
632 treatment plants also use anaerobic digesters which collect CH₄ for eventual combustion, but may have
633 fugitive CH₄ emissions. Of the urban sources of CH₄, this source is perhaps the most uncertain (Hopkins
634 et al., 2016a). For the purposes of this study, we assume CH₄ emissions are most likely to arise from the
635 plants with the largest daily flow capacity; however, emissions could also potentially arise from various
636 points of collection and/or drainage of wastewater and sewage.

637 **5.2.1.1 Wastewater Treatment Plants (Vista-LA Layer)**

638 *Data sources:*

639 The final Vista-LA wastewater treatment plant layer (IPCC – 4D1 and 4D2) relies on data from the State
640 Water Resources Control Board Facility Report Tool (SWRCB FRS), SCAG 2012 land use dataset,
641 Google Earth and Esri Basemap aerial imagery. The Vista-LA wastewater treatment plant dataset
642 provides accurate location, extent, and facility level metrics for the largest domestic wastewater treatment
643 plants in SoCAB.

644 *Data processing, validation and limitations:*

645 From the SWRCB FRS, we obtained information for wastewater treatment plants in the LA Basin for
646 2016, including facility names, addresses, coordinates, and the design flow rate in million gallons per day.
647 The raw data, which contained information on 152 plants for the state of California, 36 of which were
648 located within SoCAB, 26 which contained design flow metrics. We geocoded the CARB data as points,
649 and found many uncertainties in geolocation of wastewater treatment plants. Because of the relatively
650 small number of plants with metrics in SoCAB, we were able to successfully resolve this uncertainty.



651 We generated polygons and validated plant geolocation for the 26 SoCAB wastewater treatment plants
652 using Google Earth and Esri Basemap aerial imagery and SCAG 2012 land use data. SCAG data was
653 used to first obtain facility spatial extents. The SCAG land use code 1433, (“liquid waste disposal
654 facilities”), was used to verify locations and determine the spatial extent of the original list of wastewater
655 treatment plants. In total, 189 polygons were classified with this land use code. 44 of those polygons were
656 directly matched with point locations from the SWRCB FRS dataset. Since some facilities had multiple
657 polygons associated to them, they had to be manually merged in order to associate one polygon with one
658 wastewater treatment facility. After this merging procedure, 44 polygons were merged to 11 polygons
659 that directly matched the location of 11 SWRCB FRS wastewater treatment plants. Polygons for the other
660 15 plants were digitized using both Google Earth and Esri Basemap imagery as reference for spatial
661 extent. Each of the 26 plants was successfully validated using aerial imagery. During the manual
662 validation procedure, attention was given to identifying features such as spreading grounds, aeration
663 fields, water injection plants, and circular tanks. EPA FRS data for the year 2013 was used as a verification
664 source and contains information about wastewater treatment plants operating within petroleum refineries
665 and power plants (U.S. Environmental Protection Agency, 2016).

666 The ten additional plants from the SWRCB FRS dataset were not included in the final Vista-LA dataset
667 because they did not contain facility level metrics and design flow rates, only location information.
668 Additionally, it is difficult to identify sub-facility plant infrastructure since aerial imagery can only
669 provide a certain degree of context.

670 *Results:*

671 The final Vista-LA wastewater treatment plant layer contains geolocations for 26 wastewater treatment
672 plant facilities. Five of these wastewater treatment plants were found to be co-located with power plants.
673 The metadata contains information about the station name, design flow rate metrics, recalculated
674 locational coordinates of each facility, and validation notes including any changes made and date of last
675 update.



676 **6 Discussion**

677 **6.1 Vista-LA Data Summary**

678 The Vista-LA database consists of 33,353 individual features as points, lines and polygons among thirteen
679 spatial layers, providing a spatial representation of major CH₄ production sources in SoCAB (Figure 2).
680 For the nine polygon layers, Vista-LA depicts the true spatial extent of each facility, a major advance over
681 the original source data. Pipelines are represented as lines, and oil and gas wells are represented as points,
682 which we consider to be the most accurate representation of these sources. The remaining two sources
683 currently represented by points— dairies and anaerobic lagoons— require future work to accurately
684 describe their spatial extents.

685 The maps in Figures 3-5 show the spatial distributions of potential sources of CH₄ in the IPCC Level 1
686 categories: Energy (1), Agriculture (3), and Waste (4), respectively. The highest density of CH₄ emitting
687 infrastructure is located in the western portion of SoCAB in Los Angeles and Orange Counties (Figure
688 2). The Energy sector, specifically oil and gas wells, account for the majority of the spatial inventory
689 (32,537 features) and are primarily located in southern and northwestern Los Angeles County and
690 northern Orange County (Figure 3). The Agriculture sector is dominated by dairies and cattle farms
691 located in the Chino and San Jacinto Basins of San Bernardino and Riverside Counties (Figure 4). By
692 contrast, landfills and wastewater treatment plants are relatively evenly distributed throughout SoCAB
693 (Figure 5).

694 In total, Vista-LA polygons cover 117 km², or 0.68% of the 17,108km² extent of SoCAB, substantially
695 narrowing the area over which surveys for fugitive and not-inventoried CH₄ sources should be carried
696 out. This spatial structure more closely matches the “hotspot” nature of atmospheric CH₄ that has been
697 observed in SoCAB at the scale of meters to kilometers (Hopkins et al., 2016b) than is represented by
698 existing gridded products such as CALGEM (10 km x10 km; Jeong et al., 2013) and EPA/Harvard (0.1°
699 x 0.1°; Maasackers et al., 2016).



700 **6.2 Vista-LA Data Completeness and Uncertainty**

701 The goal of Vista-LA is to provide a complete representation of potential anthropogenic CH₄ emission
702 sources in SoCAB; however, ensuring complete spatial coverage of important CH₄ sources is challenging.
703 We made the simplifying assumption that including the eight IPCC Level 3 sources which constitute
704 ~99% of the expected California GHG inventory emissions would capture the most important CH₄
705 sources in SoCAB, omitting rice cultivation, imported electricity, and coal mining which are not present
706 in the domain (Figure 1). We also added two new source types that are not included in the California
707 GHG inventory: compressed natural gas (CNG) fueling stations (total: 109 locations) and liquefied
708 natural gas (LNG) fueling stations (total: 27 locations). While these sources are not presently included in
709 the inventory, there was sufficient evidence for fugitive CH₄ emissions for inclusion in Vista (e.g., Figure
710 8; Clark et al., 2017; Hopkins et al., 2016b), particularly given that SoCAB contains 32% and 57% of the
711 state's CNG and LNG fueling stations, respectively.

712
713 We verified our list of included source categories against the key source categories at the national level
714 from the U.S. EPA inventory (EPA, 2016), and found that rice cultivation and coal mining were the only
715 source types contributing >1% of total emissions that were not included. We also compared Vista's source
716 categories to observations of CH₄ hotspots in Los Angeles. The known sources of enhanced CH₄ levels—
717 landfills, cattle, water treatment, power plants, CNG fueling, natural gas pipelines, oil refineries, and oil
718 fields— corresponded to Vista layers with the exception of geologic seeps. This correspondence suggests
719 that Vista-LA is well suited for source attribution of anthropogenic CH₄ hotspots in SoCAB.

720
721 We omitted several categories that might have important contributions to CH₄ emissions in SoCAB, such
722 as transportation. Although transportation produces ~1% of California inventoried CH₄ emissions (and
723 <0.3% of national emissions; EPA, 2016), it likely comprises a greater fraction of SoCAB emissions
724 given the greater density of traffic in the region. We have chosen not to include a spatial layer for
725 transportation in this version of Vista—we view Vista as primarily a tool for attribution of large fugitive
726 CH₄ emission sources, and there is no evidence for this type of emission from conventionally fueled
727 vehicles. Fugitive CH₄ emissions detected along roadways are more likely to originate from leaks in



728 natural gas pipelines that lie underneath the road surface (Chamberlain et al., 2016). Adding a spatial
729 layer for transportation would be simple to achieve, such as by including a map of the road network or
730 from an existing high resolution inventory such as Hestia (Rao et al., *in review*), and needs to be included
731 in an emissions inventory.

732

733 We also omitted two possible natural sources of CH₄ emissions in SoCAB—geologic seeps and
734 wetlands—because they are not included in the most recent version of the California GHG Inventory
735 (geologic seeps are inventoried as “excluded” sources). These sources have not been included in this
736 version of Vista despite the large observed emissions from geologic seeps in SoCAB (Farrell et al., 2013;
737 Hopkins et al., 2016b). We have identified possible spatial datasets to include in future versions of Vista
738 (USGS maps of Natural Oil and Gas Seeps in California, <https://walrus.wr.usgs.gov/seeps/> and U.S. Fish
739 and Wildlife Service National Wetlands Inventory, <https://www.fws.gov/wetlands/>). There is a potential
740 that either sources may contribute significantly to the SoCAB emissions budget—we anticipate including
741 these in future versions.

742

743 There is also uncertainty in the spatial representation of sources in Vista-LA. We assumed that the spatial
744 location of sources by linking facility-level (or pipeline-, or oil well-level) datasets to IPCC source
745 categories (Table 1), although there may not be a perfect correspondence between mappable infrastructure
746 and these sources. An alternative approach would have been to map out the lifecycle of each IPCC Level
747 1 sector (e.g., Energy, Agriculture, Waste), and determine spatial locations of each lifecycle phase in the
748 domain. We chose the IPCC approach because is more standardized, and hence applicable to other cities.
749 The lifecycle approach requires local knowledge, and is likely to differ among cities and regions (Hopkins
750 et al., 2016a). We also assumed that most CH₄ emissions come from the main facility associated with an
751 emitting activity, such as wastewater treatment plants for wastewater emissions, rather than the sewer
752 network. This assumption may not hold true, for example when manure is exported from dairies and
753 treated elsewhere. In contrast to waste and agriculture, we included a higher level of detail for the natural
754 gas system because there is more evidence of quantitatively significant CH₄ emissions from distributed
755 parts of the network (e.g., pipelines).



756

757 Finally, we recognize error inherent in the availability of data, and in the original data sources themselves.
758 Vista-LA relies on publicly available datasets. Consequently, we are constrained by (a) lack of data on
759 some infrastructure types that may be transient or has never been collected, such as the locations of
760 manure piles; (b) unavailability of proprietary data, such as the locations of petroleum storage tanks or
761 gathering pipelines; and (c) data that poses a security risk, and hence cannot be distributed, such as
762 specific locations of natural gas compressor stations and high pressure transmission pipelines. Within the
763 datasets themselves, we found errors in geolocation and missing facilities. As described in the text, we
764 took steps to control these errors inherent to the source datasets by performing visual validation and using
765 multiple datasets for the same source category. In most original datasets, geolocation of some facilities
766 was incorrect by up to several kilometers for various reasons, and some geolocations corresponded to the
767 offices or street address of facilities rather than actual facility location (e.g., for dairies). Raw datasets for
768 landfills, natural gas processing plants, and wastewater treatment plants also had coarse spatial resolution
769 resulting in uncertain geolocations, which we corrected. However, we were unable to visually validate all
770 sources, including oil wells and landfills. With respect to omission of CH₄ emitting facilities, in many
771 cases, the total number of facilities varied among the raw datasets that were used to construct the Vista-
772 LA layers (e.g., landfills, natural gas processing plants, natural gas storage fields, power plants, and
773 wastewater treatment plants). For power plants, there are many small facilities in California (around 4,020
774 plants) that are not included in the EIA dataset (110 plants). Overall, these small power plant facilities
775 only represent about 3% of the total statewide electricity production related fossil fuel CO₂ emissions,
776 and therefore most are not tracked. Some of these facilities are also not grid-tied, but are facilities that
777 generate electricity for an industrial process (K. Gurney, *personal communication*). We found that at
778 least nine power plants were located within the bounds of a petroleum refinery facility in SoCAB. We
779 have not considered potential emissions from smaller facilities or those contained within other facilities,
780 but this may be important to consider as part of future work.



781 **6.3 Vista-LA Applications**

782 At present, Vista-LA does not contain the bottom-up empirical measurements required for the creation of
783 an accurate fine-scale CH₄ inventory (as in Lyon et al., 2015). However, making and interpreting
784 atmospheric CH₄ measurements is easier for the dense, heterogeneous landscape of SoCAB with the
785 guidance of the Vista-LA spatial layers. Vista-LA represents a much-needed first step towards the
786 development of a fine-scale urban CH₄ emissions inventory that can be used for design and interpretation
787 of CH₄ hotspot surveys. Importantly, Vista-LA compliments the tiered remote sensing observation
788 strategies for regional top-down CH₄ emission measurements. Figure 6 summarizes potential applications
789 of Vista-LA, which are described in the following sections.

790 **6.3.1 Research Planning**

791 Vista-LA is already in use as a planning tool for research aimed toward better understanding CH₄
792 emissions in SoCAB, through guiding design of CH₄ super-emitters surveys and appropriate selection of
793 locations for stationary CH₄ monitoring. Figure 7 shows how Vista-LA has been used for planning
794 airborne remote sensing campaigns to survey CH₄ point sources. Guidance from Vista-LA allows airborne
795 campaigns to be designed for maximum coverage of key infrastructure identified in SoCAB. In Figure 7,
796 aircraft flight lines shown in green illustrate a path optimized for coverage of key CH₄ infrastructure in
797 SoCAB.

798 **6.3.2 CH₄ Hotspot Detection**

799 In addition, Vista-LA can be used to interpret observations of atmospheric CH₄ measurements, addressing
800 the challenge of source attribution of CH₄ hotspots detected in airborne and ground-based surveys.
801 Pinpointing the source of fugitive CH₄ emissions sources in dense mixed-land use urban areas has been
802 an ongoing challenge (Cambaliza et al., 2015; Hopkins et al., 2016b). In many urban areas, many potential
803 CH₄ sources are located in close proximity, such as in the Ports of Los Angeles and Long Beach, which
804 contain extensive fossil fuel use and transportation, active oil drilling and refining, and wastewater
805 treatment. Figure 8 shows an overlay of CH₄ observations from a mobile CH₄ survey in June 2013, where



806 high frequency in situ CH₄ observations were made from a moving van, as described in Hopkins et al.
807 (2016b). Atmospheric CH₄ levels are shown as colored boxes with an “x” in the center, with blue colors
808 representing near background levels, and warmer colors (red) representing elevated CH₄. The same region
809 was flown by the Hyperspectral Thermal Emission Spectrometer (HyTES) in July 2014. Plumes of CH₄
810 were retrieved from HyTES radiance data, and are shown in green (Hulley et al., 2016). In the scene,
811 Vista-LA shows roughly a dozen oil and gas wells and a CNG fueling station near the elevated CH₄
812 observations, narrowing down the number of potential sources greatly. Together with wind direction,
813 these observations plus Vista-LA enable attribution to the facility level.

814 **6.3.3 Stakeholder and Public Engagement Tool**

815 Vista-LA also has the potential to guide CH₄ mitigation efforts by identifying persistent CH₄-emitting
816 infrastructure when combined with atmospheric measurements. In order to control CH₄ emissions
817 effectively in cities, it is essential to understand the fine-scale spatial distribution of stationary sources
818 from a broad range of industries in the energy, agriculture, and waste sectors. Local regulators and city
819 planners may be able to use the location information presented in Vista-LA, combined with targeted
820 surveys or observations, to develop enhanced CH₄ monitoring and mitigation strategies for their cities.
821 Vista-LA may also be extensible to air-quality mitigation efforts. For example, some processes that emit
822 CH₄ also result in co-emission of other gases that are important for climate and air quality. By
823 incorporating new information in Vista, such as information on permitting and/or sub-facility
824 infrastructure information, users may be able to evaluate the air quality co-benefits associated with
825 fugitive CH₄ mitigation strategies.

826 **6.4 Future Directions: Vista CH₄ Database**

827 Vista-LA was primarily developed to identify CH₄ emitting infrastructure in SoCAB. However, we
828 anticipate our approach could be scaled to other regions and over larger spatial scales, including the state
829 of California, the contiguous U.S., and possibly internationally. Expanding the Vista-LA database across
830 the state of California is highly feasible given that our framework is consistent with how the State of
831 California reports CH₄ emissions. Additionally, many of the raw data sources used in the development of



832 Vista-LA already encompass state-level or national-level spatial extents (Table 1). In theory, the approach
833 could also be expanded to any region on Earth, as long as an IPCC (or similar) inventory and geolocation
834 data for the top-emitting sources are publicly available. Our framework is also dependent on the
835 availability of timely, reliable public datasets. In this regard, Los Angeles and the state of California are
836 perfect testbeds for development. By contrast, many regions may not have such information available
837 publicly, especially in developing nations.

838 Efforts to expand the database could be enhanced by the use of automated feature extraction techniques.
839 For example, the use of automated feature extraction techniques could expedite the process of identifying,
840 extracting, and updating relevant infrastructure features. Automated feature extraction involves machine-
841 learning algorithms used to recognize patterns through image processing (see e.g., Yuan, 2016;
842 Castelluccio et al., 2015). In this way, aerial imagery in the SoCAB could essentially be used to parse
843 through and precisely locate features such as converted landfills, oil and gas wellheads, anaerobic lagoons,
844 and/or wastewater treatment plants. Future work may benefit from the use of automated feature
845 recognition algorithms using software such as eCognition, ERDAS IMAGINE, GeoMedia, InterIMAGE,
846 RemoteView and SOCET GXP in order to identify and update spatial information for facilities and
847 sources not yet known or housed in current publicly available databases.

848 In the future, the information in the Vista-LA could be used generate a high-resolution bottom-up gridded
849 CH₄ emissions product for SoCAB. While the initial goal of the Vista-LA database was to provide facility
850 location information, some of the facility- and sub-facility-level activity and operation information
851 contained within the metadata may also be useful for assigning emission factors to each source (see
852 Metadata in the Supplementary Information). For example, the Vista-LA dairy layer contains information
853 on herd population by type, which could be used to estimate emissions factors for enteric fermentation
854 and manure management. Manure management practices are known to vary widely by region, even within
855 the state of California. Potentially, the information in the Vista-LA database could also be combined with
856 top-down observations and provide independent validation of bottom-up CH₄ flux estimates, in a similar
857 approach to that shown in Section 6.2.2. In general, utilizing the spatial information in Vista-LA to assign
858 CH₄ emissions estimates could significantly minimize errors in the spatial representation of sources



859 compared to previous estimates for this region. Updates such as changes to locations, spatial extents, and
860 removal or addition of facilities will be required on at least an annual basis to provide timely and accurate
861 emissions information.

862 **7 Data availability**

863 The final Vista-LA datasets and associated metadata are open access and are available in the Oak Ridge
864 National Laboratory Distributed Active Archive Center for Biogeochemical Dynamics (ORNL DAAC)
865 (Carranza et al., 2017; <https://doi.org/10.3334/ORNLDAAC/1525>).

866 **8 Conclusions**

867 Vista-LA adopts a GIS-based approach to map CH₄ emissions in dense-mixed-land use areas like the
868 South Coast Air Basin. Characterizing CH₄ emissions at the urban scale is incredibly complex, as there
869 exist thousands of structures known to be associated with CH₄ emissions. Vista-LA successfully identifies
870 33,503 potential CH₄ emitters from three IPCC sectors: Energy, Agriculture, and Waste. Vista-LA
871 contains accurate and validated spatial extent information for nine sources including compressed natural
872 gas fueling stations, liquefied natural gas fueling stations, landfills, natural gas compressor stations,
873 natural gas storage fields, natural gas processing plants, petroleum refineries, power plants, and
874 wastewater treatment plants. It also includes point location of anaerobic lagoons, dairies, and oil and gas
875 wells as well as a natural gas pipeline network for SoCAB. Vista-LA has been assisted in flight planning
876 for CH₄ airborne campaigns, can be used in potential CH₄ hotspot detection, and can essentially be merged
877 with top-down flux estimates for the identification of individual point sources. In this way, Vista-LA
878 represents a first step towards developing a gridded emissions spatial product that can illustrate spatial
879 distribution of CH₄ emissions at a fine-scale. By fusing Vista-LA, automated surface feature recognition,
880 and other various remote sensing point source data products, we could dramatically improve the
881 attribution of methane emissions.

882 Vista-LA serves as a prototype resource to aide in the development of high-resolution bottom-up gridded
883 models of GHG emissions in densely populated urban areas with a complex variety of sources and can
884 be adapted to larger scales in accordance to characteristics innate to each respective region. The



885 development of spatially-resolved carbon emission datasets can offer significant advances in
886 understanding, managing, and mitigating carbon emissions from cities. Generally, uncertainties in
887 emission sources and their locations in inventories hinder the implementation of mitigation policies. To
888 be useful, CH₄ emissions information is needed at the scale of individual sources. In addition to accurate
889 and timely spatial information, urban CH₄ emissions inventories should also be flexible enough to
890 incorporate new information, while remaining relevant for observation-based research efforts such as
891 surveys, hotspot detection, and inversion modeling. Finally, the information should be communicated in
892 an open-source, transparent, and well-documented manner.

893 **Acknowledgements**

894 A portion of this research was carried out at the Jet Propulsion Laboratory, California Institute of
895 Technology, under contract with the National Aeronautics and Space Administration (NASA). The
896 NASA DEVELOP program (<http://develop.larc.nasa.gov/>) provided the primary support for this project
897 for VC and TR during 2015. IFV also participated in the NASA DEVELOP program and received support
898 from the NASA Scholars Program and the Minority University Research and Education (MUREP) Project
899 during 2014-2016. FMH was supported by an appointment to the NASA Postdoctoral Program at the Jet
900 Propulsion Laboratory, California Institute of Technology, administered by Universities Space Research
901 Association under contract with NASA. KRV was supported by the National Institutes of Standards and
902 Technologies (NIST) Greenhouse Gas and Climate Science Measurements Program. The authors are very
903 thankful to Dr. Ben Holt, G. Miller, and C. Rains from the NASA/JPL DEVELOP program for helpful
904 discussions regarding data analysis, and to M. Limb for comments on the manuscript. We are also thankful
905 for valuable advice and guidance from the California Air Resources Board (ARB) Greenhouse Gas
906 Emission Inventory Branch, including: A. Huang, L. Hunsaker, K. Eslinger, W. Widger, J. Charrier, and
907 G. Ruiz, and T. Rose, U. Prins, F. Thong and G. Bemis for assistance with data from the California Energy
908 Commission, and Edward Kashak from the Regional Water Quality Control Board, Santa Ana Region.
909 This writing has used information provided by the California Energy Commission. This writing does not
910 necessarily represent the views of the Energy Commission, its employees, or the State of California. The



911 Energy Commission and the State of California make no express or implied warranties, and assume no
912 legal liability for the information contained in this writing. © 2017. All Rights Reserved.

913 **References**

914 Asefi-Najafabady, S., Rayner, P. J., Gurney, K. R., McRobert, A., Song, Y., Coltin, K., Huang, J.,
915 Elvidge, C. and Baugh, K.: A multiyear, global gridded fossil fuel CO₂ emission data product: Evaluation
916 and analysis of results, *J. Geophys. Res. Atmos.*, 119(17), doi:10.1002/2013JD021296, 2014.

917 Brandt, A. R., Heath, G. A., Kort, E. A., O’Sullivan, F., Pétron, G., Joordan, S. M., Tans, P., Wilcox, J.,
918 Gopstein, A. M., Arent, D., Wofsy, S., Brown, N. J., Bradley, R., Stucky, G. D., Eardly, D. and Harriss,
919 R.: Methane Leaks from North American Natural Gas Systems, *Science* (80-.), 343(6172), 733–735,
920 doi:10.1126/science.1247045, 2014.

921 CalRecycle: SWIS Facility/Site Search, [online] Available from:
922 <http://www.calrecycle.ca.gov/SWFacilities/Directory/Search.aspx>, 2015.

923 Cambaliza, M. O. L., Shepson, P. B., Bogner, J., Caulton, D. R., Stirm, B., Sweeney, C., Montzka, S. a.,
924 Gurney, K. R., Spokas, K., Salmon, O. E., Lavoie, T. N., Hendricks, A., Mays, K., Turnbull, J., Miller,
925 B. R., Lauvaux, T., Davis, K., Karion, A., Moser, B., Miller, C., Obermeyer, C., Whetstone, J., Prasad,
926 K., Miles, N. and Richardson, S.: Quantification and source apportionment of the methane emission flux
927 from the city of Indianapolis, *Elementa*, 3, doi:10.12952/journal.elementa.000037, 2015.

928 CARB: California’s 2000-2012 Greenhouse Gas Emissions Inventory Technical Support Document.,
929 2014a.

930 CARB: The California Almanac of Emissions and Air Quality - 2013 Edition Rep., California Air
931 Resources Board, Sacramento, CA., 2014b.

932 CARB: California Greenhouse Gas Inventory for 2000-2013 — by Sector and Activity Electricity
933 Generation (In State) California Greenhouse Gas Inventory for 2000-2013 — by Sector and Activity.,
934 2015.



- 935 CARB: Documentation of California's 2000-2015 GHG Inventory — Index, [online] Available from:
936 http://www.arb.ca.gov/cc/inventory/doc/doc_index.php (Accessed 10 August 2016), 2016.
- 937 Carranza, V., Rafiq, T., Frausto-Vicencio, I., Hopkins, F., Verhulst, K. R., Rao, P., Duren, R. M. and
938 Miller, C. E. 2017. NACP Sources of Methane Emissions (Vista-LA), South Coast Air Basin,
939 California, USA. ORNL DAAC, Oak Ridge, Tennessee, USA.
940 <https://doi.org/10.3334/ORNLDAAC/1525>
- 941 Castelluccio, M., Poggi, G., Sansone, C. and Verdoliva, L.: Land Use Classification in Remote Sensing
942 Images by Convolutional Neural Networks, arxiv.org, cs.CV, 2015.
- 943 Chamberlain, S. D., Ingraffea, A. R. and Sparks, J. P.: Sourcing methane and carbon dioxide emissions
944 from a small city: Influence of natural gas leakage and combustion, *Environ. Pollut.*, 218, 102–110,
945 doi:10.1016/j.envpol.2016.08.036, 2016.
- 946 Chilingar, G. and Endres, B.: Environmental hazards posed by the Los Angeles Basin urban oilfields: an
947 historical perspective of lessons learned, *Environ. Geol.*, 47(2), 302–317, doi:10.1007/s00254-004-1159-
948 0, 2005.
- 949 Clark, N. N., McKain, D. L., Johnson, D. R., Wayne, W. S., Li, H., Akkerman, V., Sandoval, C.,
950 Covington, A. N., Mongold, R. A., Hailer, J. T. and Ugarte, O. J.: Pump-to-Wheels Methane Emissions
951 from the Heavy-Duty Transportation Sector, *Environ. Sci. Technol.*, 51(2), 968–976,
952 doi:10.1021/acs.est.5b06059, 2017.
- 953 Conley, S., Franco, G., Faloon, I., Blake, D., Peischl, J. and Ryerson, T.: Methane emissions from the
954 2015 Aliso Canyon blowout in Los Angeles, CA, *Science* (80-.), 351(6279), 1317–1320,
955 doi:10.1126/science.aaf2348, 2016.
- 956 Dlugokencky, E. J., Nisbet, E. G., Fisher, R. and Lowry, D.: Global atmospheric methane: budget,
957 changes and dangers, *Philos. Trans. R. Soc. London A Math. Phys. Eng. Sci.*, 369(1943), 2058–2072,
958 doi:10.1098/rsta.2010.0341, 2011.



- 959 DOE: Alternative Fuels Data Center, [online] Available from: <http://www.afdc.energy.gov/>, 2017.
- 960 DOGGR: GIS Mapping, [online] Available from:
961 <http://www.conservation.ca.gov/dog/maps/Pages/GISMapping2.aspx> (Accessed 18 June 2016), 2016.
- 962 Duren, R. and Miller, C.: Measuring the carbon emissions of megacities, *Nat. Clim. Chang.*, 2(8), 560–
963 562, 2012.
- 964 EIA: Office of Oil & Gas, Natural Gas Division Gas, Gas Transportation Information System, [online]
965 Available from:
966 https://www.eia.gov/pub/oil_gas/natural_gas/analysis_publications/ngpipeline/undrgrndstor_map.html,
967 2008.
- 968 EIA: Maps: Layer Information for Interactive State Maps, [online] Available from:
969 https://www.eia.gov/maps/layer_info-m.cfm, 2016.
- 970 EPA: FLIGHT: 2015 Greenhouse Gas Emissions from Large Facilities, [online] Available from:
971 <https://ghgdata.epa.gov/ghgp/main.do> (Accessed 18 April 2017), 2015.
- 972 EPA: Inventory of U.S. Greenhouse Gas Emissions and Sinks: 1990-2014., 2016.
- 973 European Commission Joint Research Centre: Netherlands Environmental Assessment Agency (2010)
974 Emission Database for Global Atmospheric Research (EDGAR), Release Version 4.2., [online] Available
975 from: <http://edgar.jrc.ec.europa.eu> (Accessed 4 November 2013), 2010.
- 976 Farrell, P., Culling, D. and Leifer, I.: Transcontinental methane measurements: Part 1. A mobile surface
977 platform for source investigations, *Atmos. Environ.*, 74, 422–431, doi:10.1016/j.atmosenv.2013.02.014,
978 2013.
- 979 Frankenberg, C., Thorpe, A. K., Thompson, D. R., Hulley, G., Kort, E. A., Vance, N., Borchardt, J.,
980 Krings, T., Gerilowski, K., Sweeney, C., Conley, S., Bue, B. D., Aubrey, A. D., Hook, S. and Green, R.
981 O.: Airborne methane remote measurements reveal heavy-tail flux distribution in Four Corners region.,



- 982 Proc. Natl. Acad. Sci. , 113(35), 9734–9739, doi:10.1073/pnas.1605617113, 2016.
- 983 Gioli, B., Toscano, P., Lugato, E., Matese, A., Miglietta, F., Zaldei, A. and Vaccari, F. P.: Methane and
984 carbon dioxide fluxes and source partitioning in urban areas: The case study of Florence, Italy, Environ.
985 Pollut., 164, 125–131, doi:10.1016/j.envpol.2012.01.019, 2012.
- 986 Gurney, K. R., Razlivanov, I., Song, Y., Zhou, Y., Benes, B. and Abdul-Massih, M.: Quantification of
987 fossil fuel CO₂ emissions on the building/street scale for a large US city, Environ. Sci. Technol., 46(21),
988 12194–12202, doi:10.1021/es3011282, 2012.
- 989 Gurney, K. R., Romero-Lankao, P., Seto, K. C., Hutyra, L. R., Duren, R., Kennedy, C., Grimm, N. B.,
990 Ehleringer, J. R., Marcotullio, P., Hughes, S., Pincetl, S., Chester, M. V., Runfola, D. M., Feddema, J. J.
991 and Sperling, J.: Climate change: Track urban emissions on a human scale, Nature, 525(7568), 179–181,
992 doi:10.1038/525179a, 2015.
- 993 Helfter, C., Tremper, A. H., Halios, C. H., Kotthaus, S., Bjorkegren, A., Grimmond, C. S. B., Barlow, J.
994 F. and Nemitz, E.: Spatial and temporal variability of urban fluxes of methane, carbon monoxide and
995 carbon dioxide above London, UK, Atmos. Chem. Phys., 16(16), 10543–10557, doi:10.5194/acp-16-
996 10543-2016, 2016.
- 997 Hirsch, J.: Dairies Moving Out of Inland Empire, Los Angeles Times, 2006.
- 998 Hopkins, F. M., Ehleringer, J. R., Bush, S. E., Duren, R. M., Miller, C. E., Lai, C., Hsu, Y., Carranza, V.
999 and Randerson, J. T.: Mitigation of methane emissions in cities: How new measurements and partnerships
1000 can contribute to emissions reduction strategies, Earth's Futur., 4(9), 408–425,
1001 doi:10.1002/2016EF000381, 2016a.
- 1002 Hopkins, F. M., Kort, E. A., Bush, S. E., Ehleringer, J., Lai, C., Blake, D. and Randerson, J. T.: Spatial
1003 patterns and source attribution of urban methane in the Los Angeles Basin, J. Geophys. Res. Atmos.,
1004 121(5), 2490–2507, doi:10.1002/2015JD024429, 2016b.



- 1005 Hsu, Y. K., VanCuren, T., Park, S., Jakober, C., Herner, J., FitzGibbon, M., Blake, D. R. and Parrish, D.
1006 D.: Methane emissions inventory verification in southern California, *Atmos. Environ.*, 44(1), 1–7,
1007 doi:10.1016/j.atmosenv.2009.10.002, 2009.
- 1008 Hulley, G. C., Duren, R. M., Hopkins, F. M., Hook, S. J., Vance, N., Guillevic, P., Johnson, W. R., Eng,
1009 B. T., Mihaly, J. M., Jovanovic, V. M., Chazanoff, S. L., Staniszewski, Z. K., Kuai, L., Worden, J.,
1010 Frankenberg, C., Rivera, G., Aubrey, A. D., Miller, C. E., Malakar, N. K., Tomás, J. M. S. and Holmes,
1011 K. T.: High spatial resolution imaging of methane and other trace gases with the airborne Hyperspectral
1012 Thermal Emission Spectrometer (HyTES), *Atmos. Meas. Tech.*, 9(5), 2393–2408, doi:10.5194/amt-9-
1013 2393-2016, 2016.
- 1014 IPCC: Good Practice Guidance and Uncertainty Management in National Greenhouse Gas Inventories.,
1015 2001.
- 1016 IPCC: 2006 IPCC Guidelines for National Greenhouse Gas Inventories, Ch. 4, Table 4.1., 2006.
- 1017 Jackson, R. B., Down, A., Phillips, N. G., Ackley, R. C., Cook, C. W., Plata, D. L. and Zhao, K.: Natural
1018 Gas Pipeline Leaks Across Washington, DC, *Environ. Sci. Technol.*, 48(3), 2051–2058,
1019 doi:10.1021/es404474x, 2014.
- 1020 Jeong, S., Cui, X., Blake, D. R., Miller, B., Montzka, S. A., Andrews, A., Guha, A., Martien, P., Bambha,
1021 R. P., LaFranchi, B., Michelsen, H. A., Clements, C. B., Glaize, P. and Fischer, M. L.: Estimating methane
1022 emissions from biological and fossil-fuel sources in the San Francisco Bay Area, *Geophys. Res. Lett.*,
1023 44(1), 486–495, doi:10.1002/2016GL071794, 2017.
- 1024 Kaffka, S., Barzee, T., El-Mashad, H., Williams, R., Zicari, S. and Zhang, R.: Evaluation of Dairy Manure
1025 Management Practices for Greenhouse Gas Emissions Mitigation in California. [online] Available from:
1026 [http://biomass.ucdavis.edu/wp-content/uploads/2016/06/ARB-Report-Final-Draft-Transmittal-Feb-26-](http://biomass.ucdavis.edu/wp-content/uploads/2016/06/ARB-Report-Final-Draft-Transmittal-Feb-26-2016.pdf)
1027 2016.pdf (Accessed 18 April 2017), 2016.
- 1028 Kashak, E.: Edward Kashak from California Regional Water Quality Board, Santa Ana Region personal



- 1029 communication with Francesca Hopkins, 2016.
- 1030 Kennedy, C., Steinberger, J., Gasson, B., Hansen, Y., Hillman, T., Havránek, M., Pataki, D., Phdungsilp,
1031 A., Ramaswami, A. and Villalba Mendez, G.: Greenhouse gas emissions from global cities, *Environ. Sci.*
1032 *Technol.*, 43, 7297–7302, doi:10.1021/es900213p, 2009.
- 1033 Lamb, B. K., Edburg, S. L., Ferrara, T. W., Harrison, M. R., Kolb, C. E., Townsend-Small, A., Dyck, W.,
1034 Possolo, A. and Whetstone, J. R.: Direct Measurements Show Decreasing Methane Emissions from
1035 Natural Gas Local Distribution Systems in the United States, *Environ. Sci. Technol.*, 49(8), 5161–5169,
1036 doi:10.1021/es505116p, 2015.
- 1037 Lyon, D. R., Zavala-Araiza, D., Alvarez, R. A., Harriss, R., Palacios, V., Lan, X., Talbot, R., Lavoie, T.,
1038 Shepson, P., Yacovitch, T. I., Herndon, S. C., Marchese, A. J., Zimmerle, D., Robinson, A. L. and
1039 Hamburg, S. P.: Constructing a Spatially Resolved Methane Emission Inventory for the Barnett Shale
1040 Region, *Environ. Sci. Technol.*, 49(13), 8147–8157, doi:10.1021/es506359c, 2015.
- 1041 Maasackers, J. D., Jacob, D. J., Sulprizio, M. P., Turner, A. J., Weitz, M., Wirth, T., Hight, C.,
1042 DeFigueiredo, M., Desai, M., Schmeltz, R., Hockstad, L., Bloom, A. A., Bowman, K. W., Jeong, S. and
1043 Fischer, M. L.: Gridded National Inventory of U.S. Methane Emissions, *Environ. Sci. Technol.*, 50(23),
1044 13123–13133, doi:10.1021/acs.est.6b02878, 2016.
- 1045 Marcotullio, P. J., Sarzynski, A., Albrecht, J., Schulz, N. and Garcia, J.: The geography of global urban
1046 greenhouse gas emissions: an exploratory analysis, *Clim. Change*, 121(4), 621–634, doi:10.1007/s10584-
1047 013-0977-z, 2013.
- 1048 McKain, K., Down, A., Raciti, S. M., Budney, J., Hutyra, L. R., Floerchinger, C., Herndon, S. C.,
1049 Nehr Korn, T., Zahniser, M. S., Jackson, R. B., Phillips, N. and Wofsy, S. C.: Methane emissions from
1050 natural gas infrastructure and use in the urban region of Boston, Massachusetts., 2015.
- 1051 Myhre, G., Shindell, D., Bréon, F.-M., Collins, W., Fuglestedt, J., Huang, J., Koch, D., Lamarque, J.-F.,
1052 Lee, D., Mendoza, B., Nakajima, T., Robock, A., Stephens, G., Takemura, T. and Zhan, H.:



1053 Anthropogenic and Natural Radiative Forcing: In *Climate Change 2013: The Physical Science Basis.*
1054 *Contribution of Working Group I to the Fifth Assessment Report of the Intergovernmental Panel on*
1055 *Climate Change*, in Cambridge University Press, Cambridge, United Kingdom and New York, NY, USA,
1056 pp. 659–740., 2013.

1057 Newman, S., Xu, X., Gurney, K. R., Hsu, Y. K., Li, K. F., Jiang, X., Keeling, R., Feng, S., O’Keefe, D.,
1058 Patarasuk, R., Wong, K. W., Rao, P., Fischer, M. L. and Yung, Y. L.: Toward consistency between trends
1059 in bottom-up CO₂ emissions and top-down atmospheric measurements in the Los Angeles megacity,
1060 *Atmos. Chem. Phys.*, 16(6), 3843–3863, doi:10.5194/acp-16-3843-2016, 2016.

1061 Oda, T. and Maksyutov, S.: A very high-resolution (1km×1km) global fossil fuel CO₂ emission inventory
1062 derived using a point source database and satellite observations of nighttime lights, *Atmos. Chem. Phys.*,
1063 11(2), 543–556, doi:10.5194/acp-11-543-2011, 2011.

1064 Olivier, J. and Peters, J.: CO₂ from non-energy use of fuels: A global, regional and national perspective
1065 based on the IPCC Tier 1 approach, *Resour. Conserv. Recycl.*, 45(3), 210–225, 2005.

1066 Patarasuk, R., Gurney, K. R., O’Keefe, D., Song, Y., Huang, J., Rao, P., Buchert, M., Lin, J. C., Mendoza,
1067 D. and Ehleringer, J. R.: Urban high-resolution fossil fuel CO₂ emissions quantification and exploration
1068 of emission drivers for potential policy applications, *Urban Ecosyst.*, 19(3), 1013–1039,
1069 doi:10.1007/s11252-016-0553-1, 2016.

1070 Perata: Senate Bill No. 1368, Chapter 598. [online] Available from:
1071 http://www.energy.ca.gov/emission_standards/documents/sb_1368_bill_20060929_chaptered.pdf, 2006.

1072 Phillips, N. G., Ackley, R., Crosson, E. R., Down, A., Hutyra, L. R., Brondfield, M., Karr, J. D., Zhao,
1073 K. and Jackson, R. B.: Mapping urban pipeline leaks: Methane leaks across Boston, *Environ. Pollut.*, 173,
1074 1–4, doi:10.1016/j.envpol.2012.11.003, 2013.

1075 Pipeline and Hazardous Materials Safety Administration; U.S. Department of Transportation: National
1076 Pipeline Mapping System, [online] Available from: <https://www.npms.phmsa.dot.gov/>, 2013.



- 1077 Rao, P., Gurney, K. R., Patarasuk, R., Yang, S., Miller, C. E., Duren, R. M. and Eldering, A.: Spatio-
1078 temporal variations in on-road CO₂ emissions in the Los Angeles Megacity, AIMS Geosci., (*in review*).
- 1079 State Water Resources Control Board; California Environmental Protection Agency: Facility Reporting
1080 Service, [online] Available from:
1081 <https://ciwqs.waterboards.ca.gov/ciwqs/readOnly/CiwqsReportServlet?inCommand=reset&reportName>
1082 =RegulatedFacility/, 2016.
- 1083 Townsend-Small, A., Tyler, S. C., Pataki, D. E., Xu, X. and Christensen, L. E.: Isotopic measurements of
1084 atmospheric methane in Los Angeles, California, USA: Influence of “fugitive” fossil fuel emissions, J.
1085 Geophys. Res. Atmos., 117(7), 1–11, doi:10.1029/2011JD016826, 2012.
- 1086 U.S. Energy Information Administration: Refinery Capacity Report., 2015.
- 1087 U.S. Environmental Protection Agency: EPA Facility Registry Service (FRS): Wastewater Treatment
1088 Plants, Data.Gov [online] Available from: [https://catalog.data.gov/dataset/epa-facility-registry-service-](https://catalog.data.gov/dataset/epa-facility-registry-service-frs-wastewater-treatment-plants)
1089 [frs-wastewater-treatment-plants](https://catalog.data.gov/dataset/epa-facility-registry-service-frs-wastewater-treatment-plants), 2016.
- 1090 Verhulst, K., Karion, A., Kim, J., Salameh, P., Keeling, R., Newman, S., Miller, J., Sloop, C., Pongetti,
1091 T., Rao, P., Wong, C., Hopkins, F. M., Yadav, V., Weiss, R. F., Duren, R. M. and Miller, C. E.: Carbon
1092 Dioxide and Methane Measurements from the Los Angeles Megacity Carbon Project: 1. Calibration,
1093 Urban Enhancements, and Uncertainty Estimates, Atmos. Chem. Phys., 17, 8313-8341,
1094 <https://doi.org/10.5194/acp-17-8313-2017>, 2017.
- 1095 Viatte, C., Lauvaux, T., Hedelius, J. K., Parker, H., Chen, J., Jones, T., Franklin, J. E., Deng, A. J., Gaudet,
1096 B., Verhulst, K. and Duren, R.: Methane emissions from dairies in the Los Angeles Basin, Atmos. Chem.
1097 Phys., 17, 7509-7528, <https://doi.org/10.5194/acp-17-7509-2017>, 2017.
- 1098 Wennberg, P. O., Mui, W., Wunch, D., Kort, E. A., Blake, D. R., Atlas, E. L., Santoni, G. W., Wofsy, S.
1099 C., Diskin, G. S., Jeong, S. and Fischer, M. L.: On the sources of methane to the Los Angeles atmosphere,
1100 Environ. Sci. Technol., 46(17), 9282–9289, doi:10.1021/es301138y, 2012.



1101 Wong, C. K., Pongetti, T. J., Oda, T., Rao, P., Gurney, K. R., Newman, S., Duren, R. M., Miller, C. E.,
1102 Yung, Y. L. and Sander, S. P.: Monthly trends of methane emissions in Los Angeles from 2011 to 2015
1103 inferred by CLARS-FTS observations, *Atmos. Chem. Phys.*, 16(20), 13121–13130, doi:10.5194/acp-16-
1104 13121-2016, 2016.

1105 Wong, K. W., Fu, D., Pongetti, T. J., Newman, S., Kort, E. A., Duren, R., Hsu, Y.-K., Miller, C. E., Yung,
1106 Y. L. and Sander, S. P.: Mapping CH₄ : CO₂ ratios in Los Angeles with CLARS-FTS from Mount Wilson,
1107 California, *Atmos. Chem. Phys.*, 15(1), 241–252, doi:10.5194/acp-15-241-2015, 2015.

1108 Wunch, D., Wennberg, P. O., Toon, G. C., Keppel-Aleks, G. and Yavin, Y. G.: Emissions of greenhouse
1109 gases from a North American megacity, *Geophys. Res. Lett.*, 36(15), 1–5, doi:10.1029/2009GL039825,
1110 2009.

1111 Yuan, J.: Automatic Building Extraction in Aerial Scenes Using Convolutional Networks, arXiv.org,
1112 cs.CV, 2016.

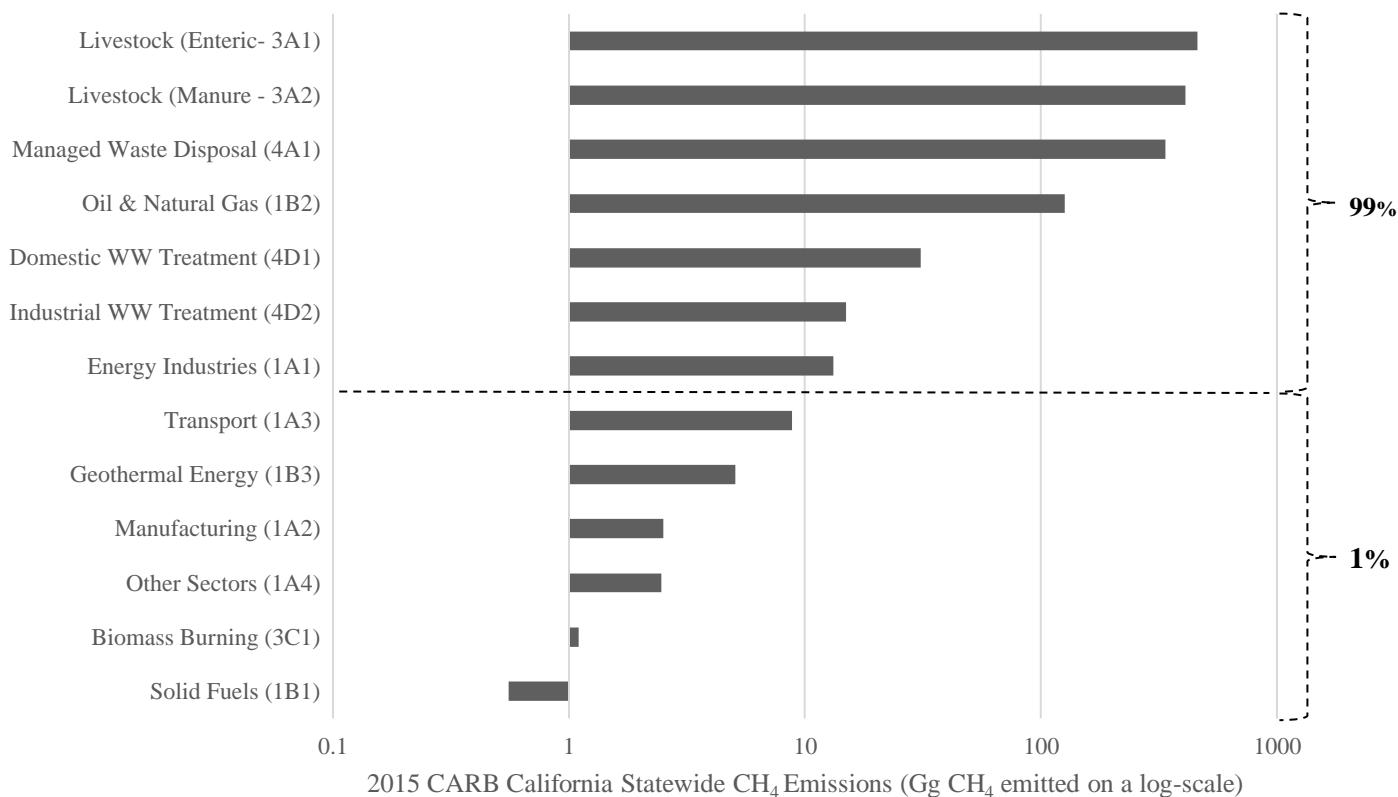
1113 Zavala-Araiza, D., Lyon, D. R., Alvarez, R. A., Davis, K. J., Harriss, R., Herndon, S. C., Karion, A., Kort,
1114 E. A., Lamb, B. K., Lan, X., Marchese, A. J., Pacala, S. W., Robinson, A. L., Shepson, P. B., Sweeney,
1115 C., Talbot, R., Townsend-Small, A., Yacovitch, T. I., Zimmerle, D. J. and Hamburg, S. P.: Reconciling
1116 divergent estimates of oil and gas methane emissions, *Proc. Natl. Acad. Sci.*, 112(51), 15597–15602,
1117 doi:10.1073/pnas.1522126112, 2015.

1118



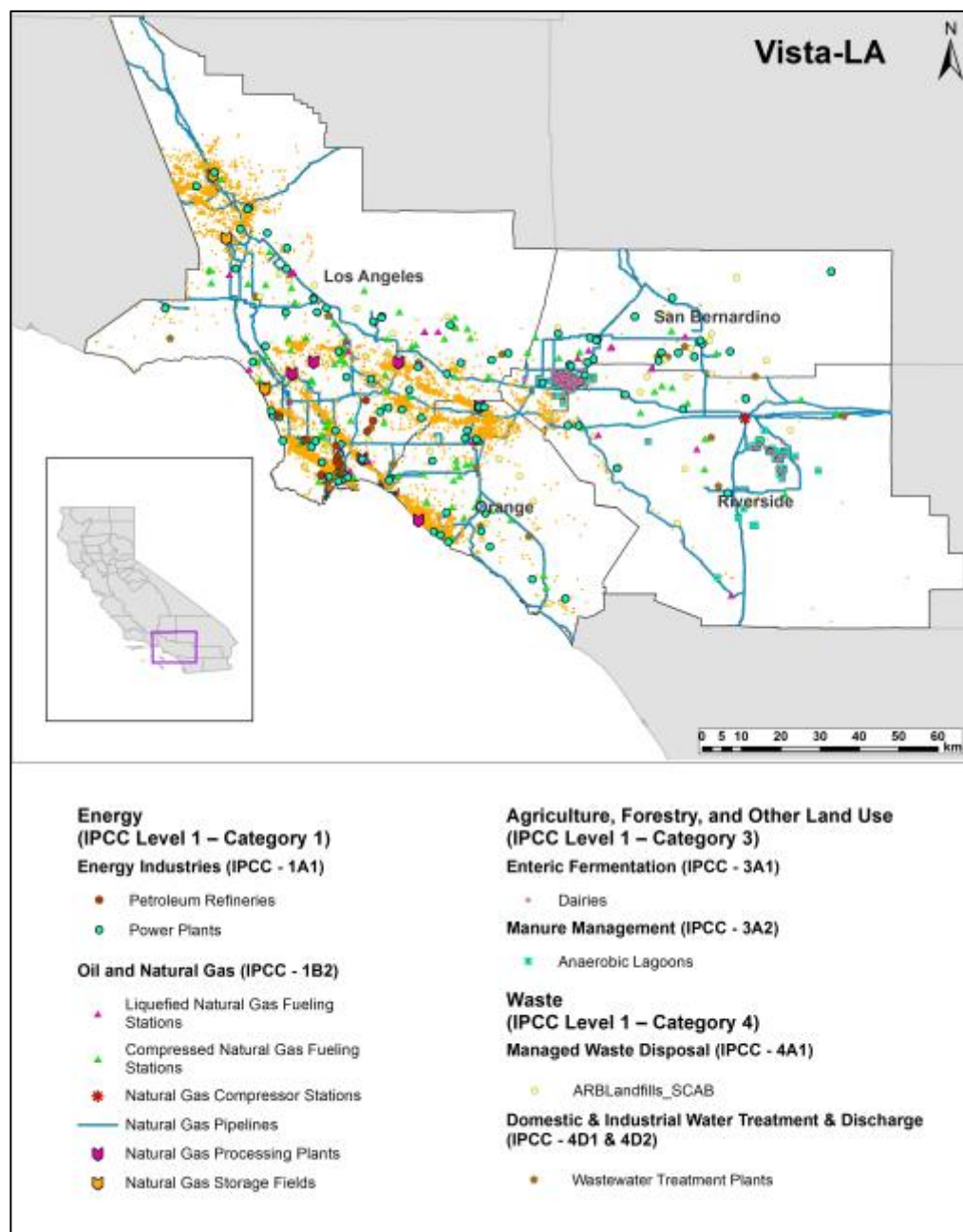
1119 **Figures**

1120



1121

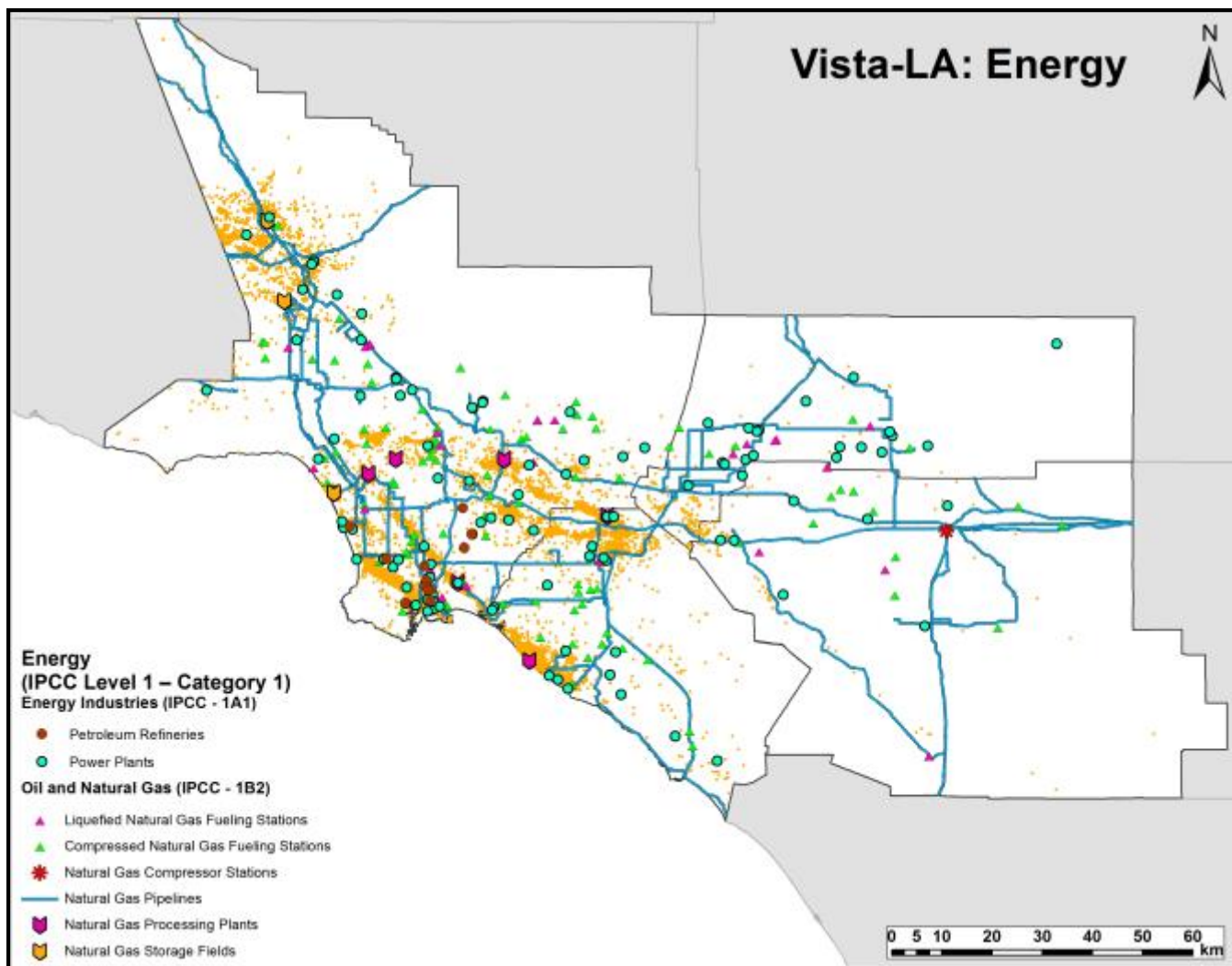
1122 **Figure 1: Ranking of inventoried California CH₄ emissions for 2015 by IPCC Level 3 categories.** This graph plots the
 1123 total emitted Gg of CH₄ for each IPCC sector on a logarithmic scale as calculated by CARB for the year 2015. This data is
 1124 based on IPCC Level 3 categories which are indicated in parenthesis. Only the top 13 of the 35 IPCC Level 3 categories are
 1125 shown for clarity. The total 2015 emission from these 13 sectors was 1,412.91 Gg CH₄. Emissions from activities that are non-
 1126 existent in the South Coast Air Basin region were not considered part of the Vista-LA database and are not shown in the graph.
 1127 These activities included imported electricity (IPCC – 1A1), rice cultivation (IPCC – 3C7), and coal mining (IPCC – 1A2).
 1128 The top seven IPCC Level 3 categories encompass roughly 99% of California’s statewide CH₄ emissions (~1,392 Gg CH₄),
 1129 are also relevant to SoCAB, and are captured in the Vista-LA database. Note: WW refers to wastewater treatment plants.



1130 **Figure 2: Overview of Vista-LA.** Locations are shown for infrastructure with known or expected potential to emit CH₄ in the
 1131 South Coast Air Basin (SoCAB). Vista layers are categorized by their corresponding IPCC Level 3 from the State of California
 1132 GHG Inventory (see Table 1). Currently, compressed and liquefied natural gas fueling stations and natural gas storage fields
 1133 are not included in the statewide GHG emissions inventory, but may be a significant source of fugitive CH₄ emissions in the
 1134 SoCAB (see e.g., Conley et al., 2016; Hopkins et al., 2016b). Note: infrastructure in polygon form is difficult to distinguish
 1135 from a static zoomed-out image; however, the majority of Vista layers can be viewed at the meter-level. Exceptions to this
 1136 rule are for natural gas compressor stations and natural gas pipelines due to privacy and security concerns. Total: 33,353
 1137 features across 13 layers: 9 polygon layers; 3 point layers; 1 polyline layer.
 1138



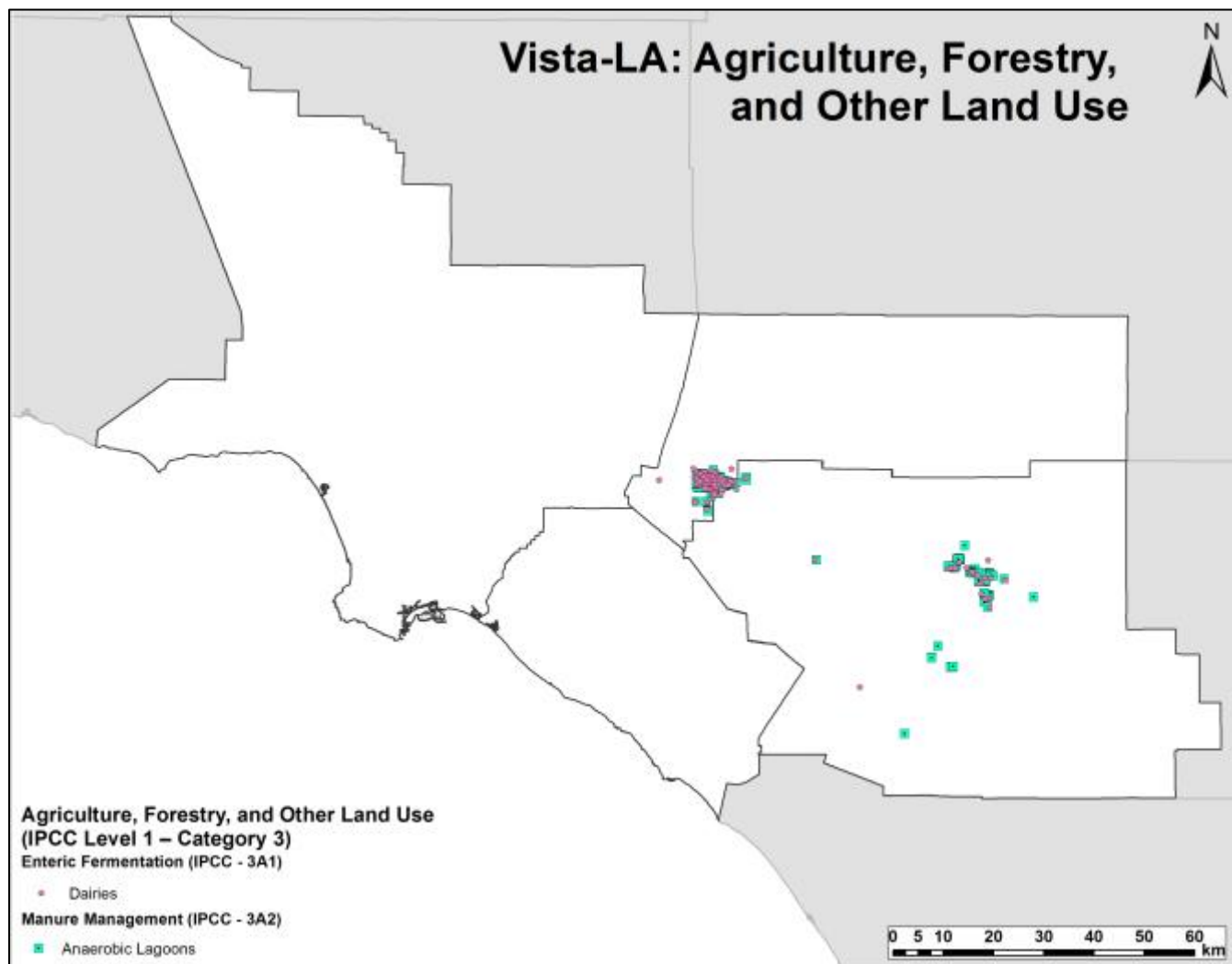
1139



1140
1141

1142 **Figure 3: Energy (IPCC Level 1 - Category 1).** Spatial distribution of infrastructure associated with the energy industry that
1143 emit CH₄ through fuel combustion (IPCC - 1A1) and/or fugitive emissions (IPCC - 1B2). Natural gas storage fields and
1144 compressed and liquefied natural gas fueling stations are currently not explicitly inventoried in the California GHG emissions
1145 inventory. Note: infrastructure in polygon form is difficult to distinguish from a static zoomed-out image; however, the
1146 majority of Vista layers can be viewed at the sub-meter level. Exceptions to this rule are for natural gas compressor stations
1147 and natural gas pipelines due to privacy and security concerns.

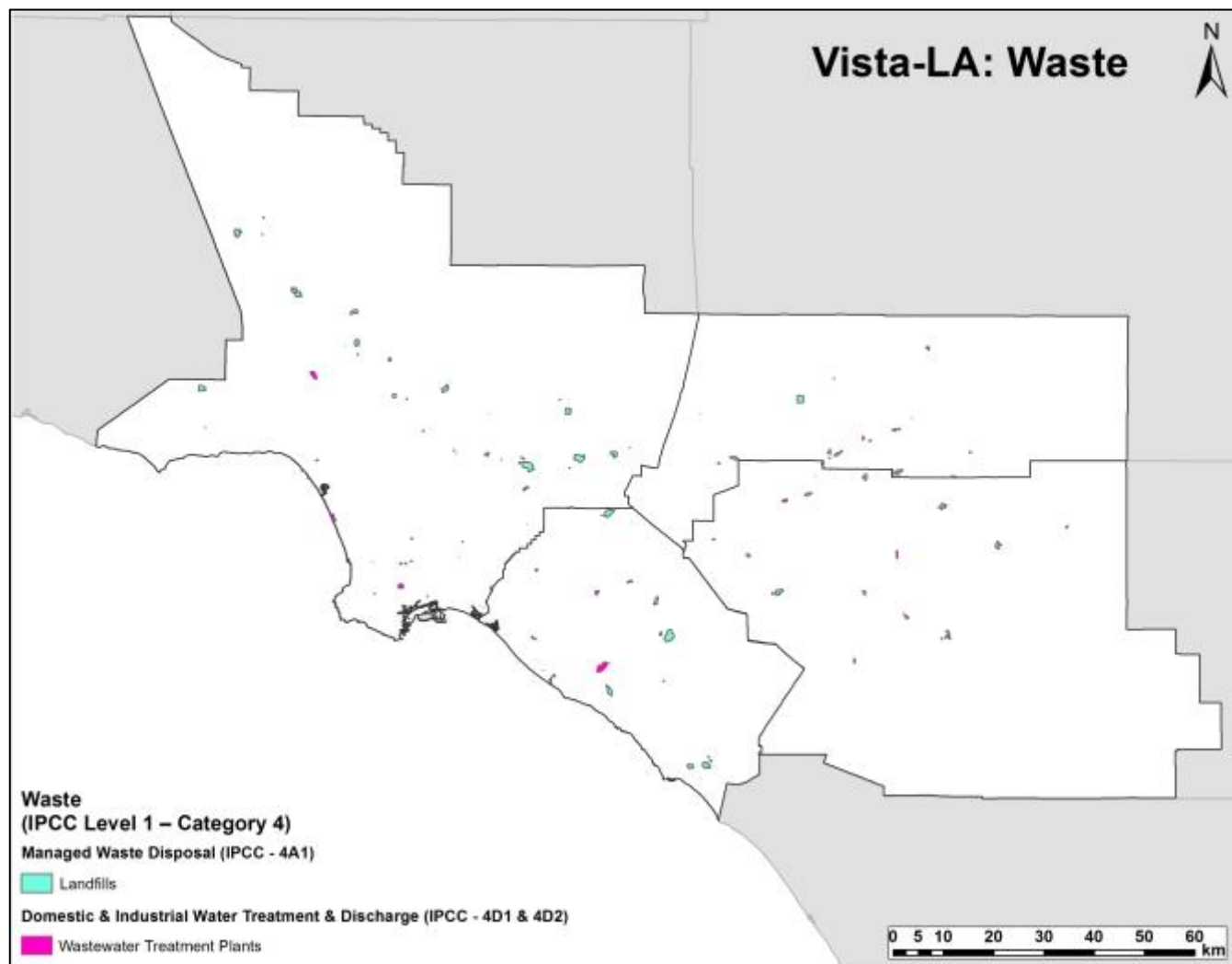
1148



1149

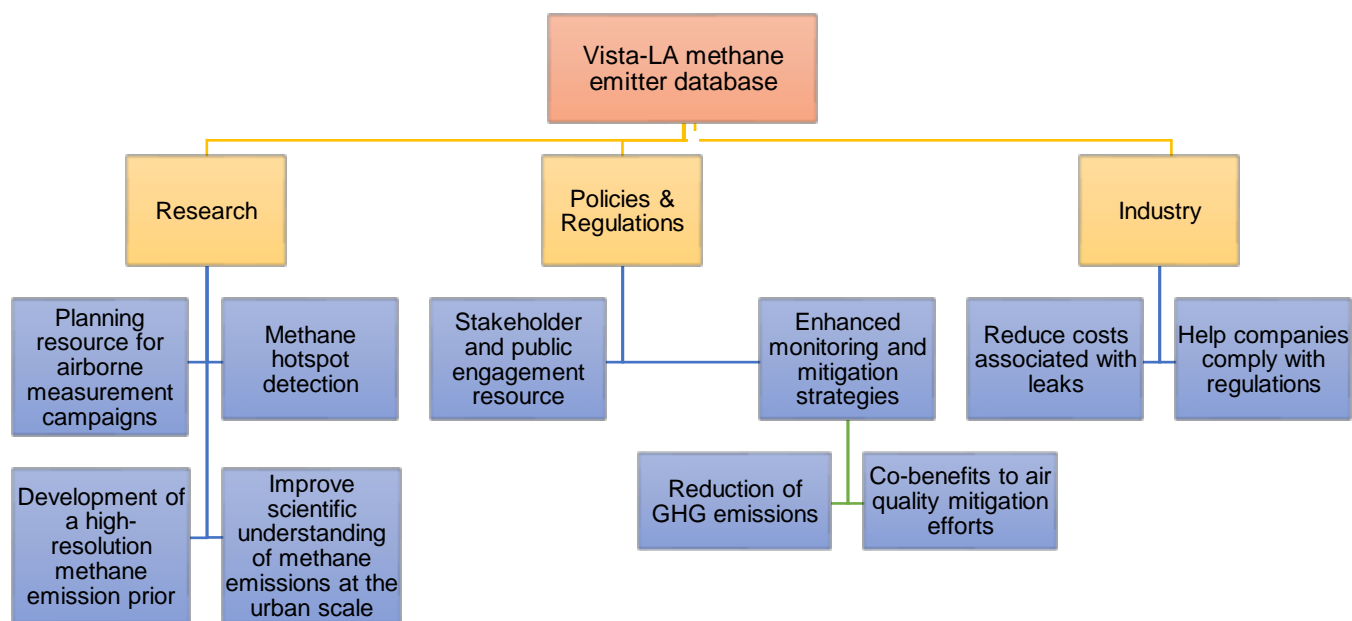
1150 **Figure 4: Agriculture, Forestry, and Other Land Use (IPCC Level 1 - Category 3).** Spatial distribution of dairies and their
1151 respective manure lagoons in the South Coast Air Basin (SoCAB), encompassing enteric fermentation and manure
1152 management CH₄ sources. The largest clusters of dairies are located in the Chino and San Jacinto regions, with 110 dairies.
1153 San Jacinto Basin was home to 22 dairies and one cattle farm and Chino housed 56 dairies, 26 cattle farms and 5 other livestock
1154 farms in the year 2015. About 228 anaerobic lagoons were identified in these two clusters.

1155

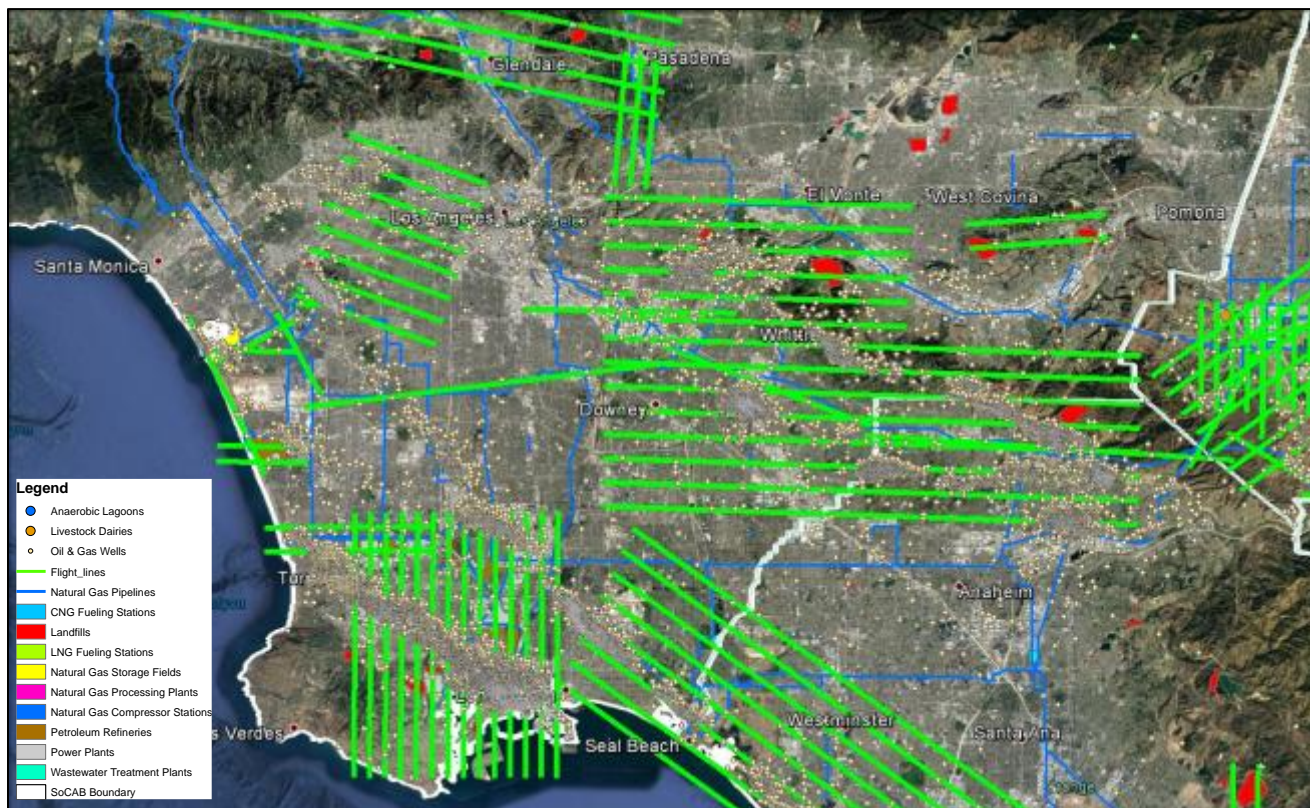


1156
1157 **Figure 5: Waste (IPCC Level 1 - Category 4).** Spatial distribution of 73 landfills and 26 wastewater treatment plants in the
1158 South Coast Air Basin (SoCAB).

1159

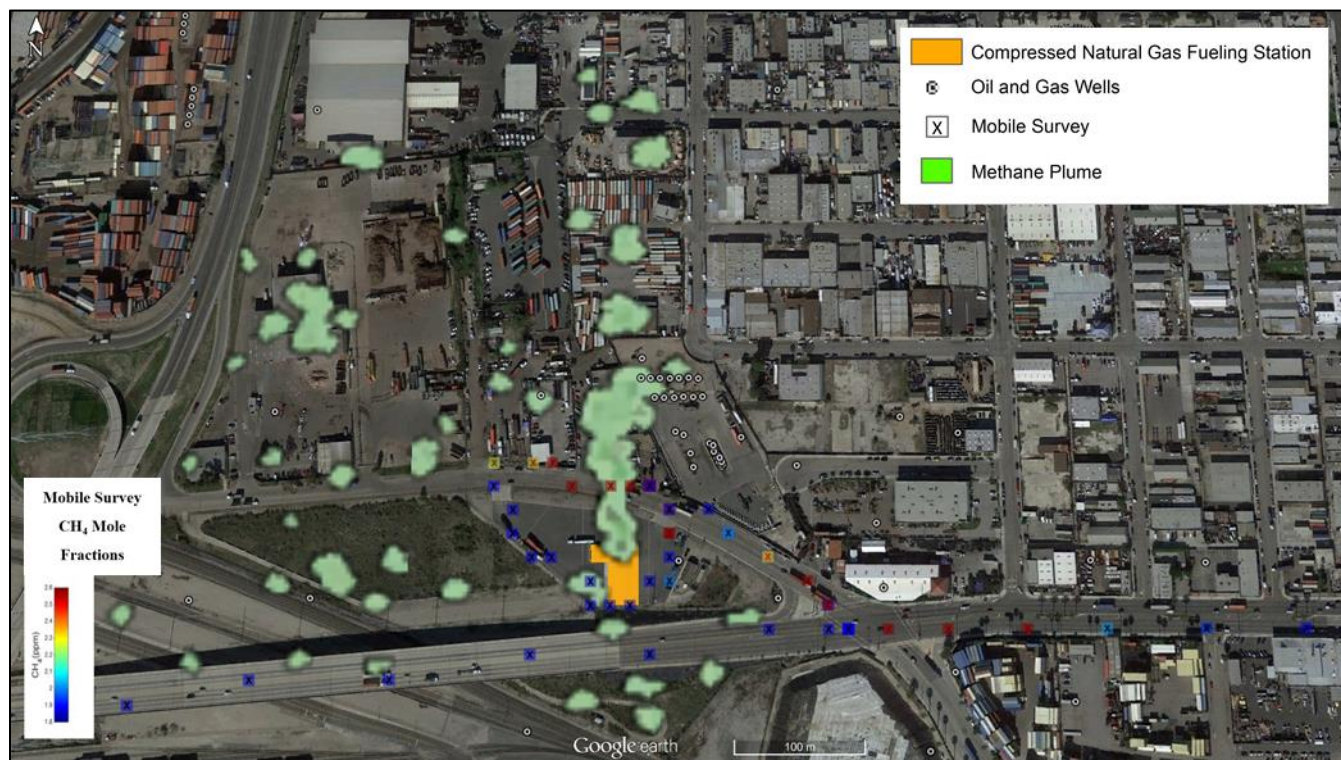


1160
1161 **Figure 6: Overview of applications of the Vista-LA CH₄ emissions mapping tool.** Vista-LA can provide numerous
1162 applications and benefits to research, policy, and industry.
1163



1164
1165
1166
1167
1168

Figure 7: Vista-LA as a flight planning resource. The flight path of an airborne CH₄ remote sensing campaign to survey CH₄ point source emissions, shown as green lines, was optimized to include CH₄ emitting infrastructure for key sources shown in Vista-LA.



1169

1170 **Figure 8: Application of Vista as a source attribution tool for CH₄ hotspots.** Vista-LA can be used to detect and determine
 1171 the source of CH₄ hotspots from on-road mobile surveys and aircraft measurements. In this example, Vista-LA layers are
 1172 shown with CH₄ plumes from airborne imaging by the HyTES instrument and atmospheric CH₄ levels from a mobile survey
 1173 in the Port of Long Beach, California. The co-location of the green colored CH₄ plume from HyTES (July 2014) and the red
 1174 point observations of enhanced CH₄ levels from the mobile survey (June 2013) suggest that the CNG fueling station, shown
 1175 as an orange polygon, is the source of observed CH₄ emissions.
 1176



1177
1179
1180
1181
1182

Tables

Table 1: Summary of Vista-LA layers. Vista-LA layers, representing CH₄ sources corresponding to IPCC Level 3, are shown organized by IPCC greenhouse gas emission reporting taxonomy. The source and year of the raw datasets, the maximum spatial coverage, number of features and format are also given for each Vista-LA layer.

CH ₄ Sector	CH ₄ Source Type	Vista-LA Layers (CH ₄ Source)	Data Source (Year)	Raw Data Spatial Coverage (Data Source)	Vista-LA No. of Features	Vista-LA Data Format
IPCC Level 1	IPCC Level 2	IPCC Level 3				
1. Energy	1A Fuel Combustion Activities	Energy Industries (IPCC - 1A1)				
		Petroleum Refineries ^a	EIA (2016) SCAG (2005, 2012)	CONUS (EIA) California (SCAG 2005, SCAG 2012)	12	polygons / kmz
		Power Plants ^a	EIA (2016) SCAG (2005, 2012)	CONUS (EIA) California (SCAG 2005, SCAG 2012)	109	polygons / kmz
	1B Fugitive Emissions From Fuels	Oil and Natural Gas (IPCC - 1B2)				
		Compressed Natural Gas (CNG) Fueling Stations ^b	U.S. DOE AFDC (2017)	CONUS	109	polygons / kmz
		Liquefied Natural Gas (LNG) Fueling Stations ^b	U.S. DOE AFDC (2017)	CONUS	27	polygons / kmz
		Natural Gas Compressor Stations ^c	EPA FLIGHT Tool (2016)	CONUS	1 ^e	polygons / kmz
		Natural Gas Pipelines ^d	CEC (2012) ^d EIA (2017)	California (CEC) CONUS (EIA)	N/A 111	N/A polylines / kmz
		Natural Gas Processing Plants	EIA (2014)	CONUS	6	polygons / kmz
		Natural Gas Storage Fields	DOGGR (2016) EIA (2016)	California (DOGGR) CONUS (EIA)	3	polygons / kmz
Oil and Gas Wells	DOGGR (2016)	California	32,537	points / kmz		
3. Agriculture, Forestry & Other Land Use	3A Livestock	Enteric Fermentation (IPCC - 3A1)				
		Dairies	RWQCB (2015)	Chino, Ontario, Riverside Areas	110	points / kmz
		Manure Management (IPCC - 3A2)				
		Anaerobic Lagoons	NASA JPL-Caltech/RWQCB (2015)	Chino, Ontario, Riverside Areas	228	points / kmz
4. Waste	4A Solid Waste Disposal	Managed Waste Disposal (IPCC - 4A1)				
		Landfills	CARB (2014) CalRecycle (2015) SCAG (2005, 2012)	California (CARB) California (CalRecycle) California (SCAG 2005, SCAG 2012)	73	polygons / kmz
	4D Wastewater Treatment & Discharge	Domestic and Industrial Water Treatment & Discharge (IPCC - 4D1 and 4D2)				
		Wastewater Treatment Plants	CARB (2016) SCAG (2005, 2012)	California (CARB) California (SCAG 2005, SCAG 2012)	26	polygons / kmz

1183
1184
1185
1186

^aSources may also include fugitive emissions that fall under IPCC source type 1B
^bSource not currently included in the California Air Resources Board's 2010-2015
 GHG Inventory.

^cOnly includes reporting facilities

^dCEC pipeline data only available as a static representation in Figures 2 and 3.

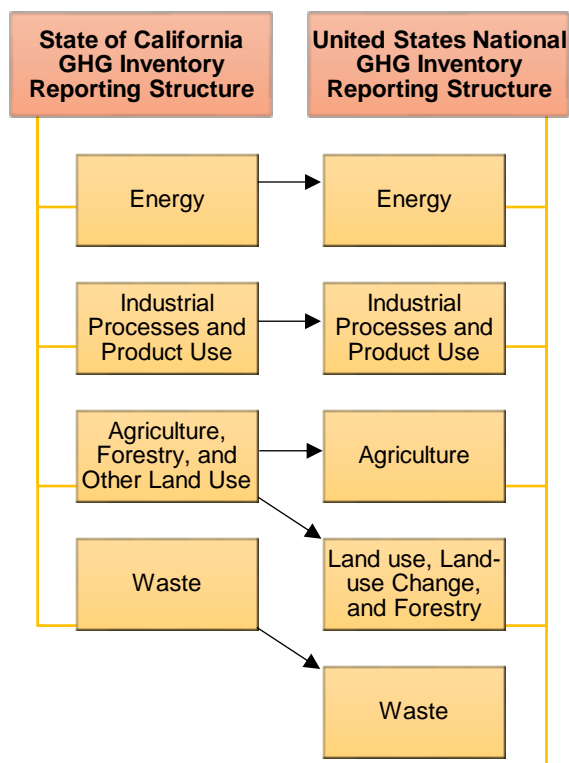


- 1189 **NOTE:**
1190 CalRecycle = California Department of Resources Recycling and Recovery
1191 CARB = California Air Resources Board
1192 CEC = California Energy Commission
1193 CONUS = Contiguous United States Region
1194 DOE = U.S. Department of Energy
1195 DOGGR = California Department of Conservation, Division of Oil, Gas, and Geothermal Resources
1196 EIA = U.S. Energy Information Administration
1197 EPA FLIGHT Tool= U.S. Environmental Protection Agency Facility Level Information on GHG Tool
1198 EPA FRS = U.S. Environmental Protection Agency Facility Registry Service
1199 NPMS = National Pipeline Mapping System
1200 RWQCB = California EPA Regional Water Quality Control Board, Santa Ana Region
1201 SCAG = Southern California Association of Governments



1202 **Appendix**

1203 **Figure A1: Comparison between GHG emissions inventory reporting structure for the State of California vs. the United**
1204 **States.** Vista-LA complies with the State of California’s GHG emissions inventory structure, but can be adapted to different
1205 regions, such as for the national GHG emissions inventory of the United States. Arrows indicate links between sector levels
1206 of the two GHG inventories.



1207

1208